Tool for Rapid Analysis of glycopeptide by Permethylation (TRAP) *via* one-pot site mapping and glycan analysis.

Asif Shajahan, Nitin T. Supekar, Christian Heiss, Mayumi Ishihara, and Parastoo Azadi*

Complex Carbohydrate Research Center, The University of Georgia, 315 Riverbend Road, Athens, GA 30602

Corresponding Author*: azadi@uga.edu

Supplementary Materials

Table of Contents

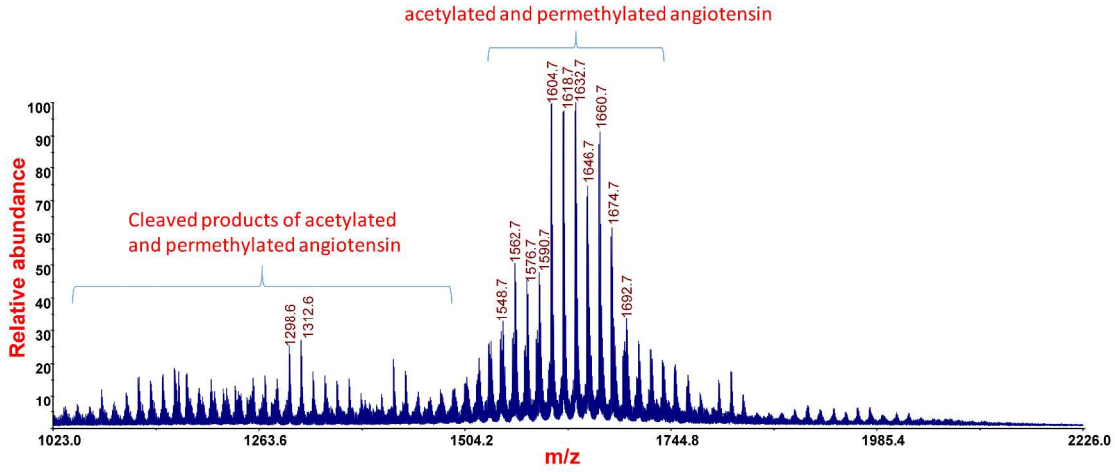

Supp. Figure S1: Cluster of peaks and cleaved products were observed for the acetylated and permethylated angiotensin on MALDI-MS, which could be due to partial acetylation of histidine and tyrosine.

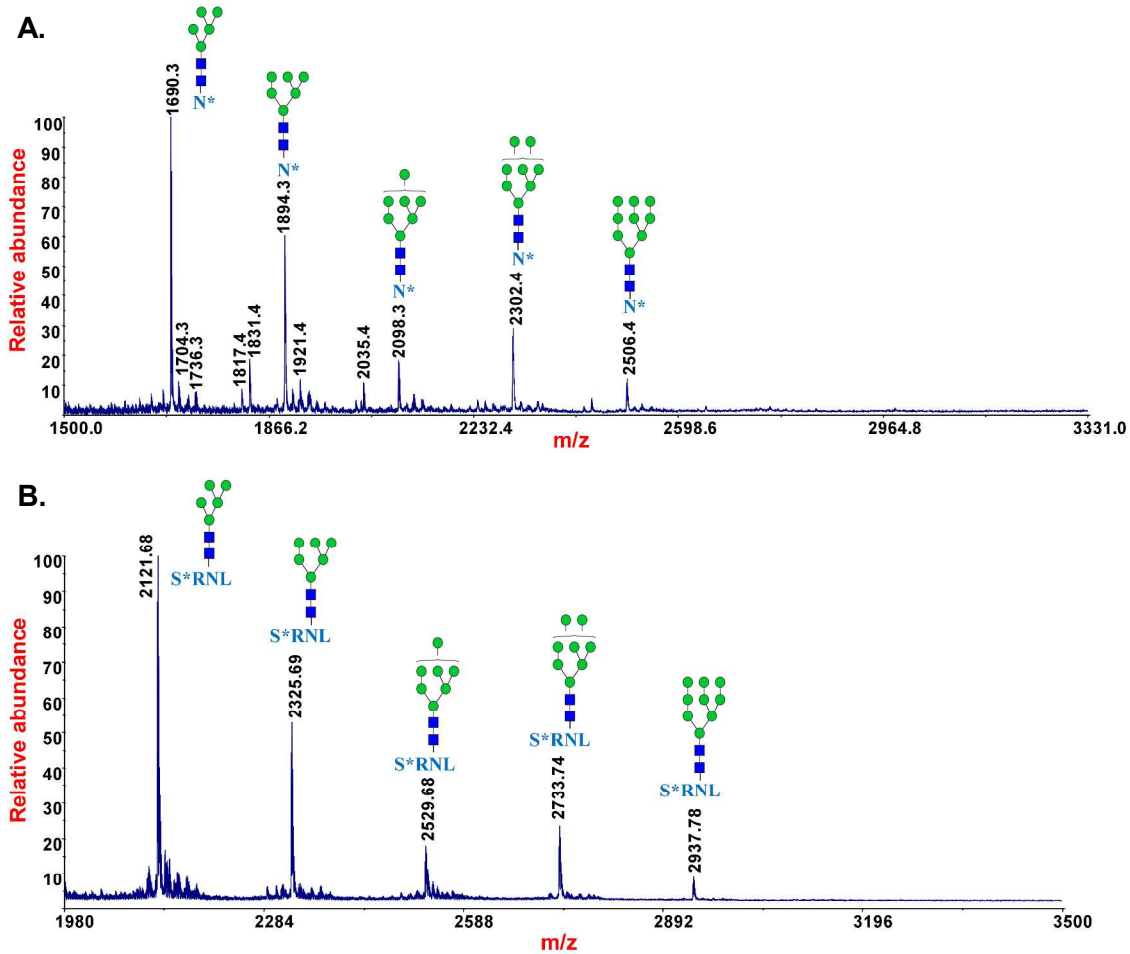

Supp. Figure S2. Analysis of pronase digest of RNase B by permethylation of glycopeptides and mass spectrometry; MALDI-MS spectra of multiple glycoforms of permethylated glycopeptide from the pronase digest of RNase B; **A.** at 1/20 pronase glycoprotein ratio; **B.** at 1/30 pronase glycoprotein ratio; S*RNL. * loss of NMe_3.

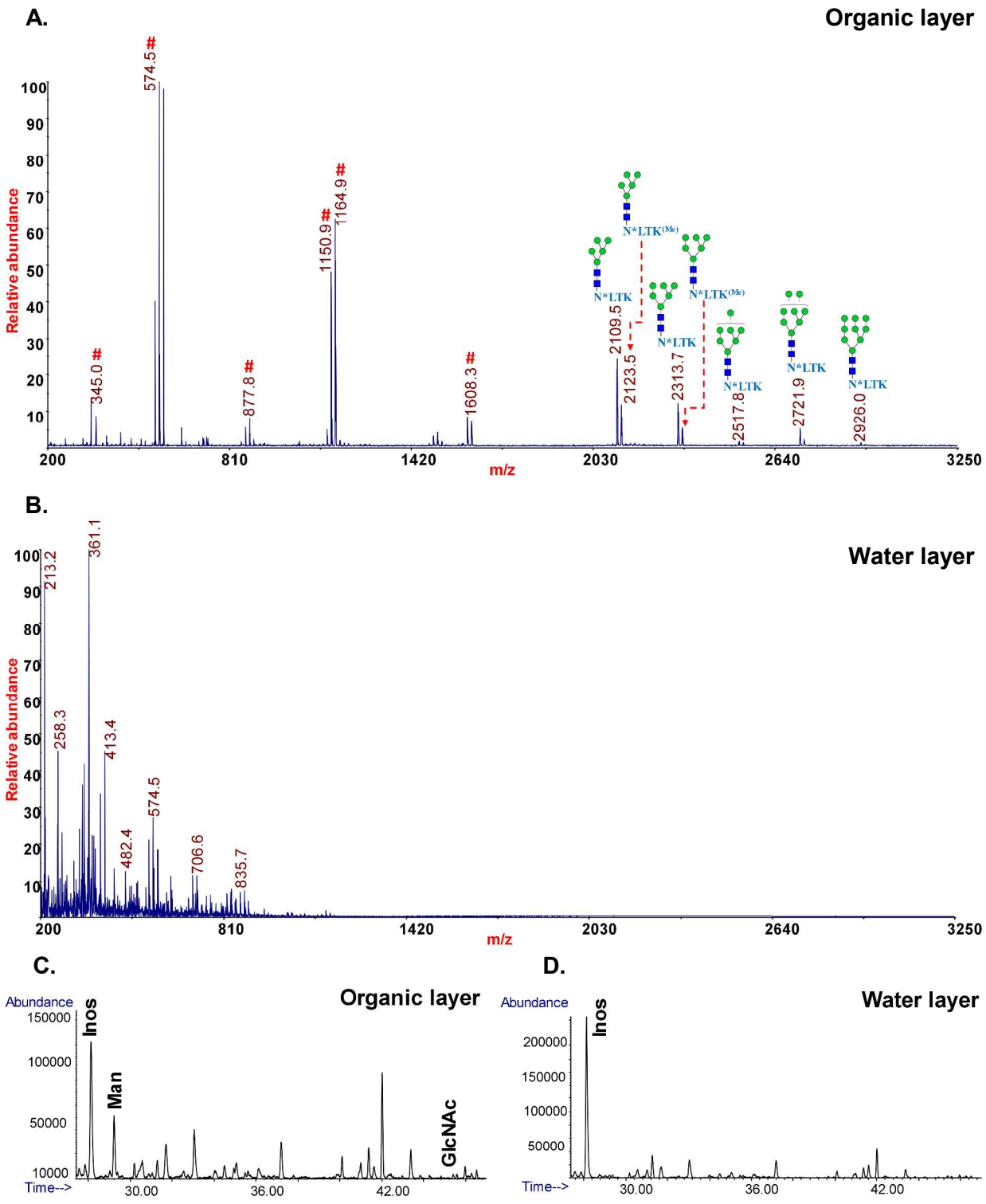
A.
Organic layer
Relative abundance
m/z
574.5 #
1164.9 #
1150.9 #
345.0 #
877.8 #
1608.3 #
2109.5
2123.5
2313.7
2517.8
2721.9
2926.0
N*LTK
N*LTK(Me)
B.
Water layer
Relative abundance
m/z
361.1
213.2
258.3
413.4
574.5
482.4
706.6
835.7
C.
Organic layer
Abundance
Time-->
Inos
Man
GlcNAc
D.
Water layer
Abundance
Time-->
Inos

Supp. Figure S3. Evaluation of reproducibility and extraction efficiency of TRAP (the figure is a representative of triplicate experiments); **A.** MALDI-MS spectrum of multiple glycoforms of permethylated glycopeptide N*LTK from the tryptic digest of RNase B extracted on organic layer, **B.** MALDI-MS spectrum of permethylated tryptic digest of RNase B extracted on water layer, **C** & **D**. monosaccharide composition analysis by GC-MS of organic and water layer, respectively. The figures demonstrate complete recovery of permethylated glycopeptide on organic layer during liquid-liquid extraction (LLE) since no peak corresponding to glycopeptides was observed in water layer. * loss of NMe_3, # non-glycopeptide peak.

Results and discussion on the evaluation of reproducibility and liquid-liquid extraction efficiency of TRAP

In order to evaluate the liquid-liquid extraction efficiency after the permethylation of glycopeptides, we have compared the presence of permethylated glycopeptide species in both organic and water layer. The organic dichloromethane layer was directly analyzed by MALDI-MS after evaporation (Supp. Figure 3A). The aqueous layer was desalted by C18 SPE, dried and analyzed by MALDI-MS (Supp. Figure 3B). The organic and aqueous layers were also analyzed for the presence of monosaccharides by GC-MS method (Supp. Figures 3C and 3D). In both analysis, almost complete recovery of permethylated glycopeptides towards the organic layer was observed. The experiment was conducted in triplicate and consistent results were observed in all cases. To evaluate the efficient retention of permethylated glycopeptide on C18 SPE cartridge, we have performed direct C18 SPE of permethylation reaction mixture after quenching the reaction with ddH_2O without dichloromethane extraction. Efficient retention of permethylated glycopeptide on C18 SPE cartridge was observed as shown in Supp. Figure S4, even with TRAP performed on 25 μg of RNase B tryptic digest.

Experimental procedure

Evaluation of LLE of permethylated glycopeptides. The permethylated glycopeptides mixture (250 μg, permethylated in triplicate) was vortexed thoroughly for 10 min with CH_2Cl_2 and the organic and aqueous layer was separated. The organic layer was washed five times with 2 mL ddH_2O. The organic layer was removed carefully and transferred to a clean glass tube and subsequently dried under a stream of nitrogen gas. The aqueous layer and the water washes was mixed, desalted by passing through C18 SPE and lyophilized. The efficiency of the extraction was evaluated by MALDI-MS and gas chromatography (GC) of both organic and water layers (Supp. Figure S3).

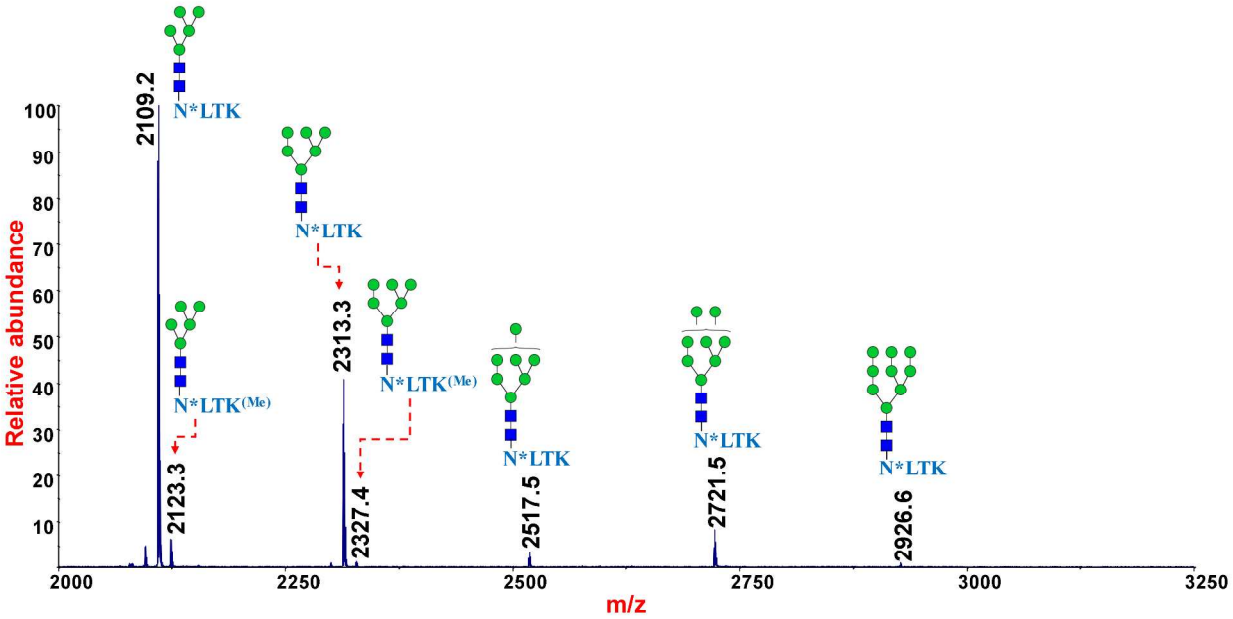

Supp. Figure S4. Analysis of tryptic digest of RNase B (25 µg) by TRAP followed by SPE sample clean up without organic extraction; MALDI-MS spectrum of multiple glycoforms of permethylated glycopeptide NLTK from the tryptic digest of RNase B. * loss of NMe_3. The spectrum also demonstrates that the sensitivity of TRAP method is 25 µg for RNase B.

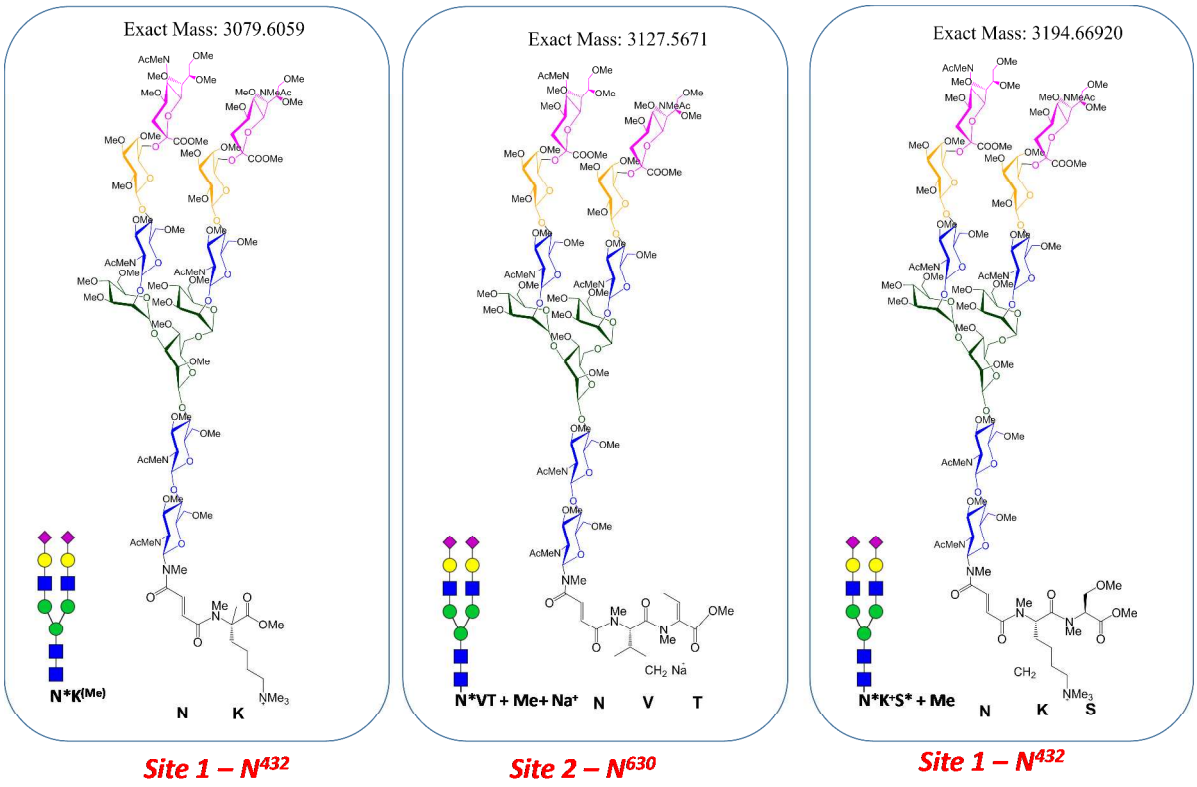

Supp. Figure S5. Structures of glycoforms of permethylated glycopeptides 'N*K$^{(Me)}$', 'N*VT+Me' and 'N*KS+Me' detected from the MS analysis of pronase digest of human transferrin.

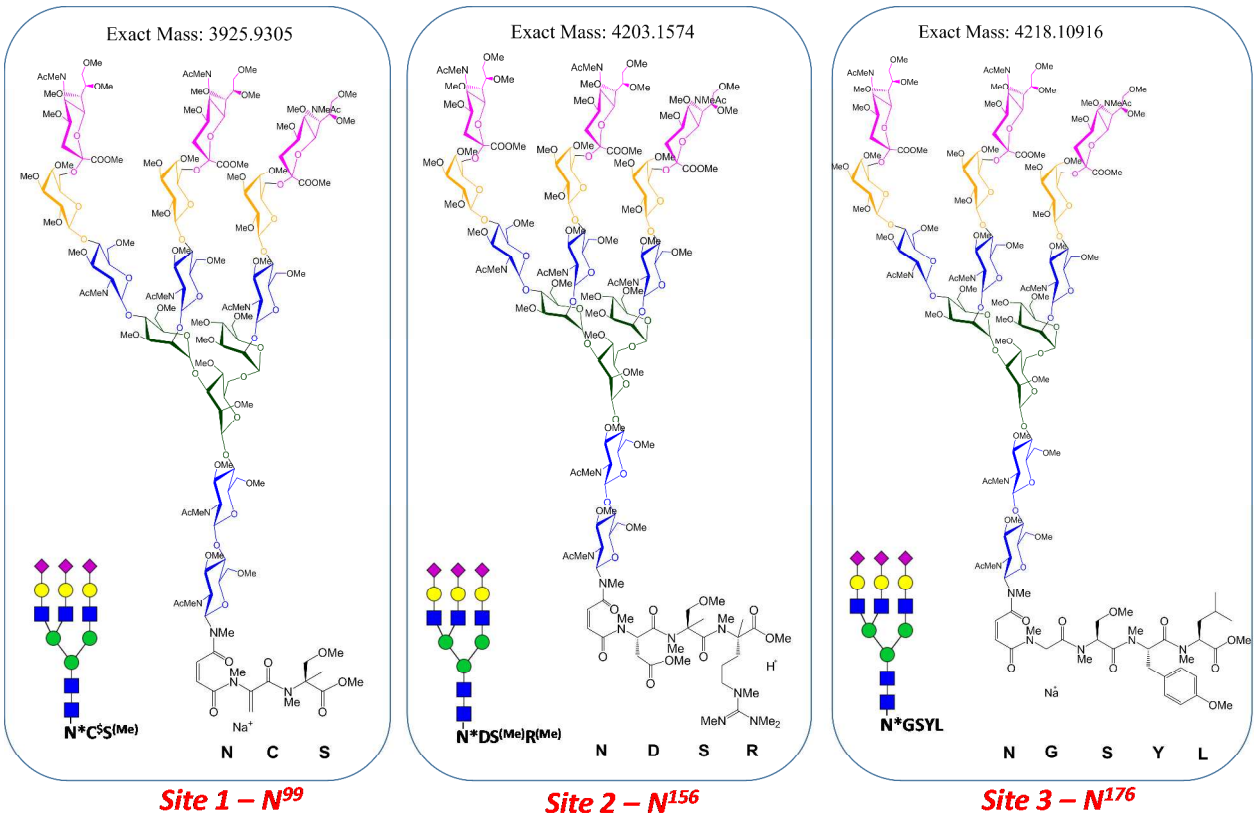

Supp. Figure S6. Structures of glycoforms of permethylated glycopeptides 'N*CS^{(Me)}$', 'N*DS$^{(Me)}R^{(Me)}$' and 'N*GSYL' detected from the MS analysis pronase digest of bovine fetuin.

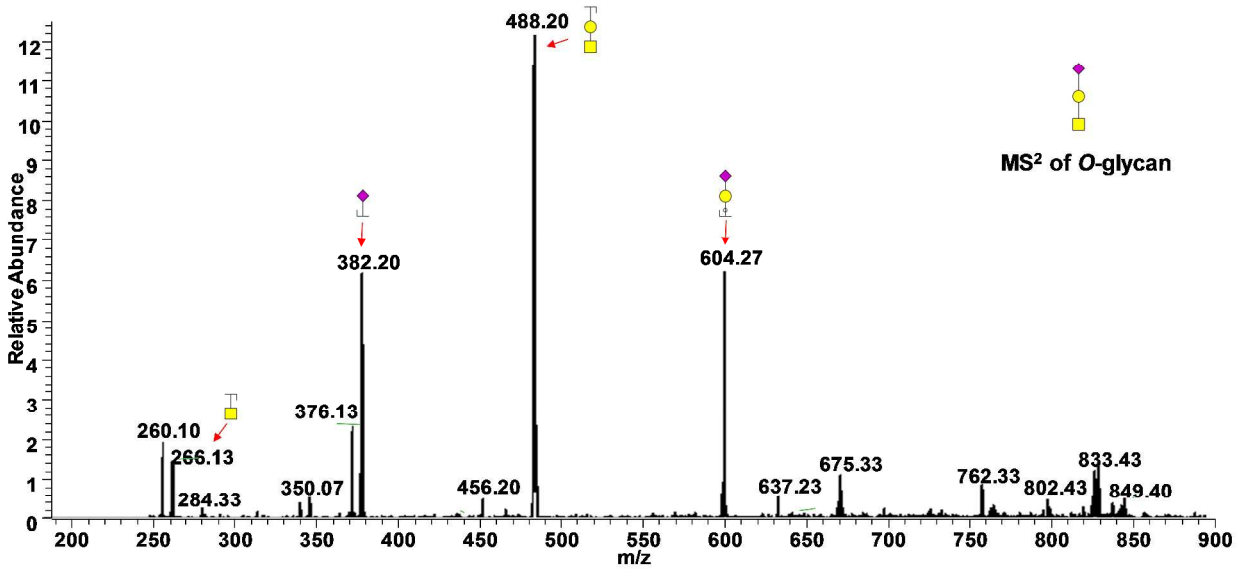

Supp. Figure S7. CID MS^2 of permethylated *O*-glycan (unreduced) from the glycopeptides of bovine fetuin upon permethylation (lithium adduct).

Modifications observed on amino acids of peptides during permethylation.

A peptide library with various peptides which comprises all 20 natural amino acids were permethylated individually and characterized by MS and MS^n experiments. In order to deduce a general rule, modifications observed on the amino acids during permethylation reaction was observed and tabulated as shown in Supp. Tables 1-17.

Supp. Table S1. Modifications observed on the amino acids upon permethylation of the peptides and glycopeptides

No.	Common name of amino acid	Structure of methylated amino acids observed	Mass difference of permethylated amino acids observed in peptides
1	Glycine	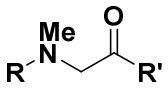 PerMe - G	102.0555
2	Alanine	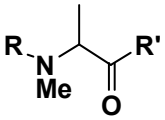 PerMe - A	116.0711
3	Serine	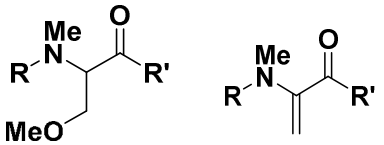 PerMe - S PerMe - S# 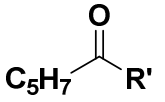 PerMe - S@#	115.0633 83.0371 95.0497
4	Threonine	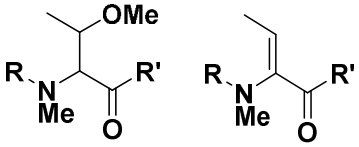 PerMe - T PerMe - T#	129.0790 97.0528
5	Cysteine	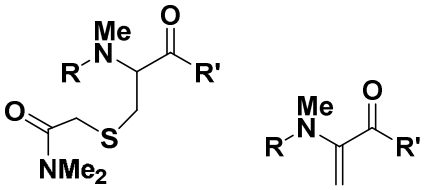 PerMe - C (IAA) PerMe - C$	202.0776 83.0371
6	Valine	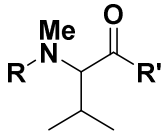 PerMe - V	113.0841

7	Leucine	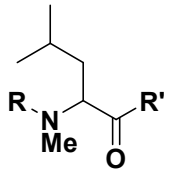 PerMe - L	127.0997
8	Isoleucine	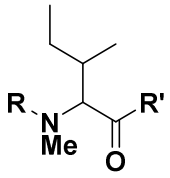 PerMe - I	127.0997
9	Methionine	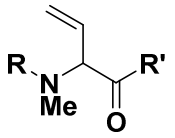 PerMe - M$	97.0528
10	Proline	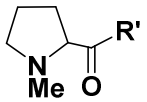 PerMe - P	174.0766
11	Phenyl alanine	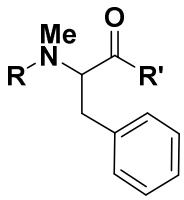 PerMe - F	161.0841
12	Tyrosine	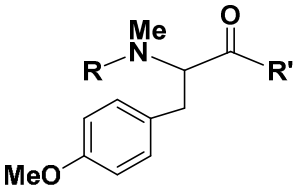 PerMe - Y	191.0946
13	Tryptophan	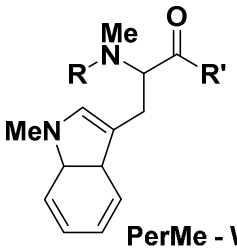 PerMe - W	216.1263
14	Aspartic acid	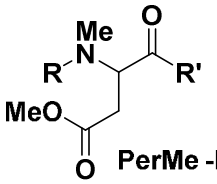 PerMe -D	143.0582

15	Glutamic acid	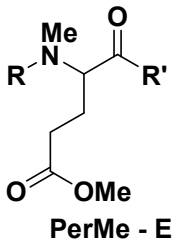 PerMe - E	157.0739
16	Asparagine	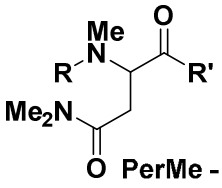 PerMe - N	156.0899
17	Glutamine	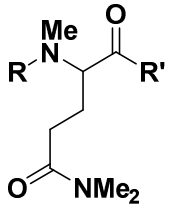 PerMe - Q	170.1055
18	Histidine	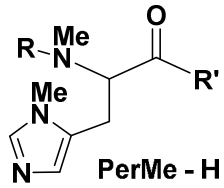 PerMe - H	165.0902
19	Lysine	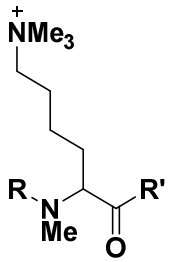 PerMe - K	185.1648
20	Arginine	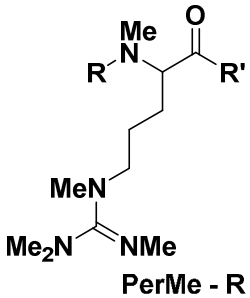 PerMe - R	226.1794
# - loss of OMe, @ - loss of NMe_3, $ - loss of SMe *Elimination of N-terminal α-amine group (after quarternization) was also observed on the peptides during permethylation*			

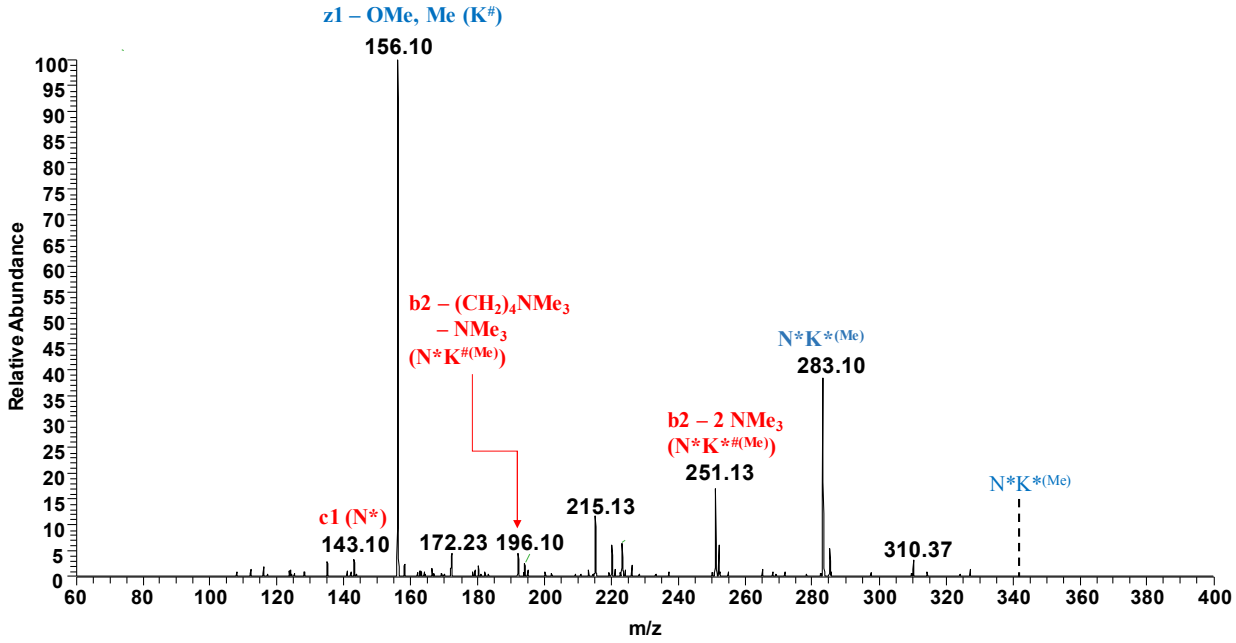

Supp. Figure S8: CID MS^3 fragmentation spectra of peptide $N^*K^{(Me)}$ (generated from the MS^2 of transferrin glycopeptide) at m/z 342.24 (1^+).

Supp. Table S2. $N^*K^{(Me)}$

Predicted fragment structure	Amino acid sequence	Fragment type
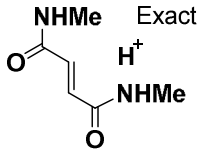 Exact Mass: 143.0815	N*	c1
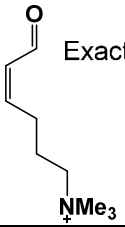 Exact Mass: 156.1383	$K^{\#}$	z1 – OMe, Me
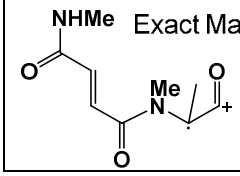 Exact Mass: 196.0842	$N^*K^{\#(Me)}$ - $(CH_2)_4NMe_3$	b2 - $(CH_2)_4NMe_3$ - NMe_3

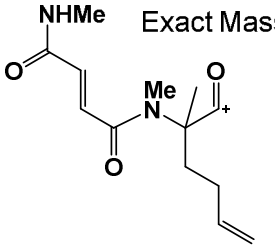	N*K*# (Me)	b2 - 2 NMe_3
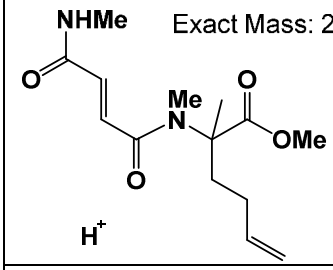	N*K* (Me)	
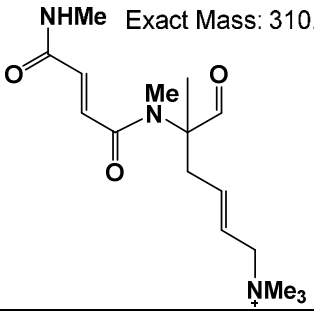	N*K#(Me)	
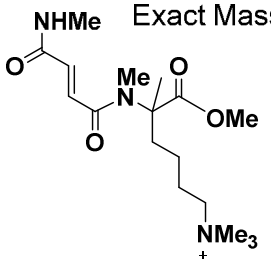	N*K(Me)	
* loss of NMe_3 # loss of OMe		

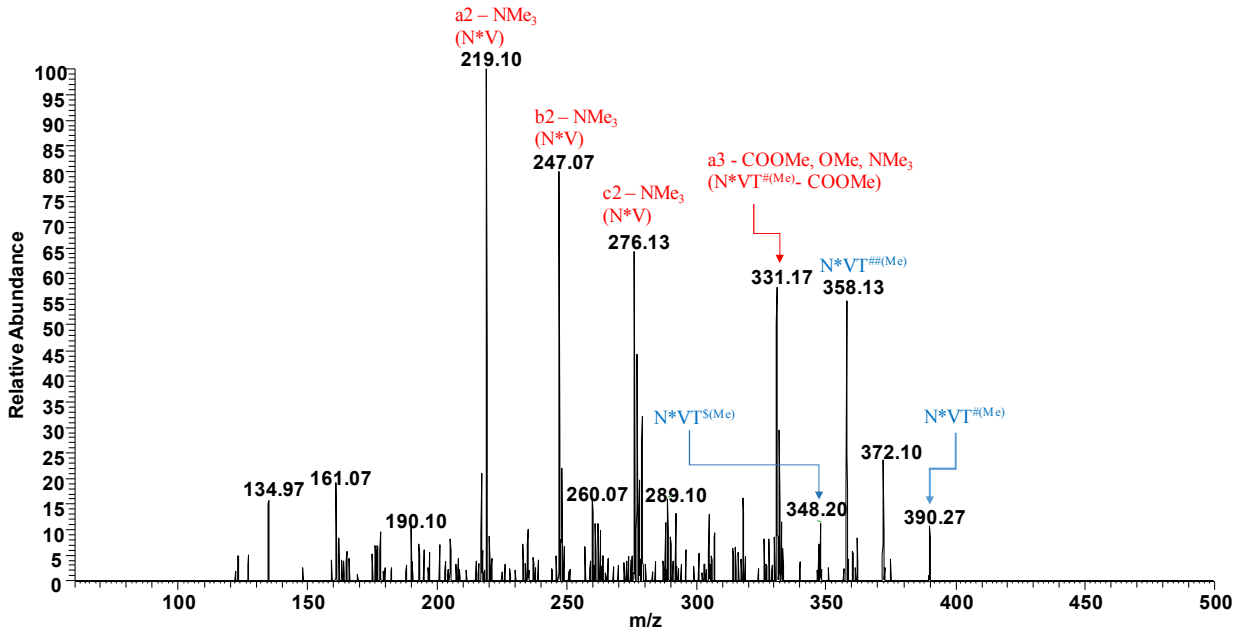

Supp. Figure S9: CID MS^3 fragmentation spectra of peptide N*VT$^{\#(Me)}$ (generated from the MS^2 of transferrin glycopeptide) at m/z 390.20 (1^+).

Supp. Table S3. N*VT$^{\#(Me)}$

Predicted fragment structure	Amino acid sequence	Fragment type
Exact Mass: 219.1104 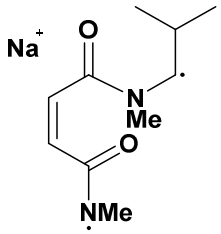	N*V	a2 - NMe_3
Exact Mass: 247.1053 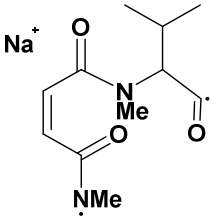	N*V	b2 - NMe_3

Exact Mass: 276.1319 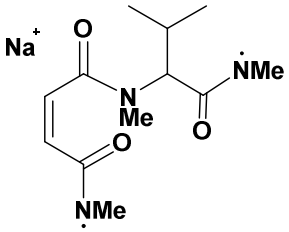	N*V	c2 - NMe_3
Exact Mass: 331.1866 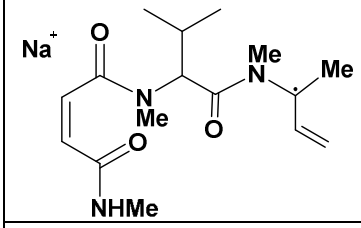	N*VT$^{\#(Me)}$ - COOMe	a3 - COOMe - OMe - NMe_3
Exact Mass: 348.1530 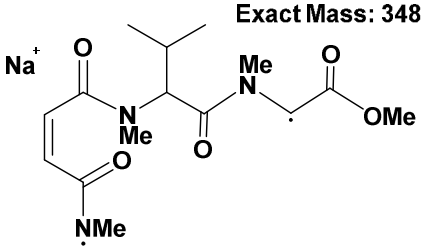	N*VT$^{\$(Me)}$	
Exact Mass: 358.1737 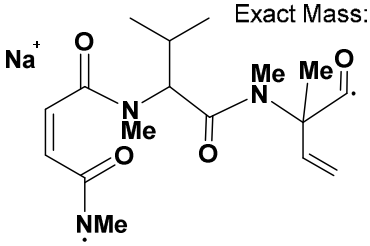	N*VT$^{\#\#(Me)}$	
Exact Mass: 390.1999 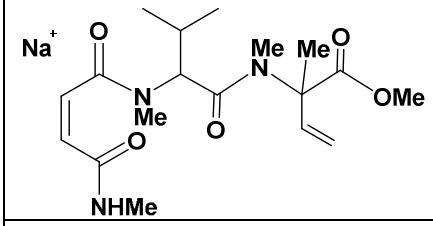	N*VT$^{\#(Me)}$	
* loss of NMe_3 # loss of OMe $ loss of $CH(OMe)CH_3$		

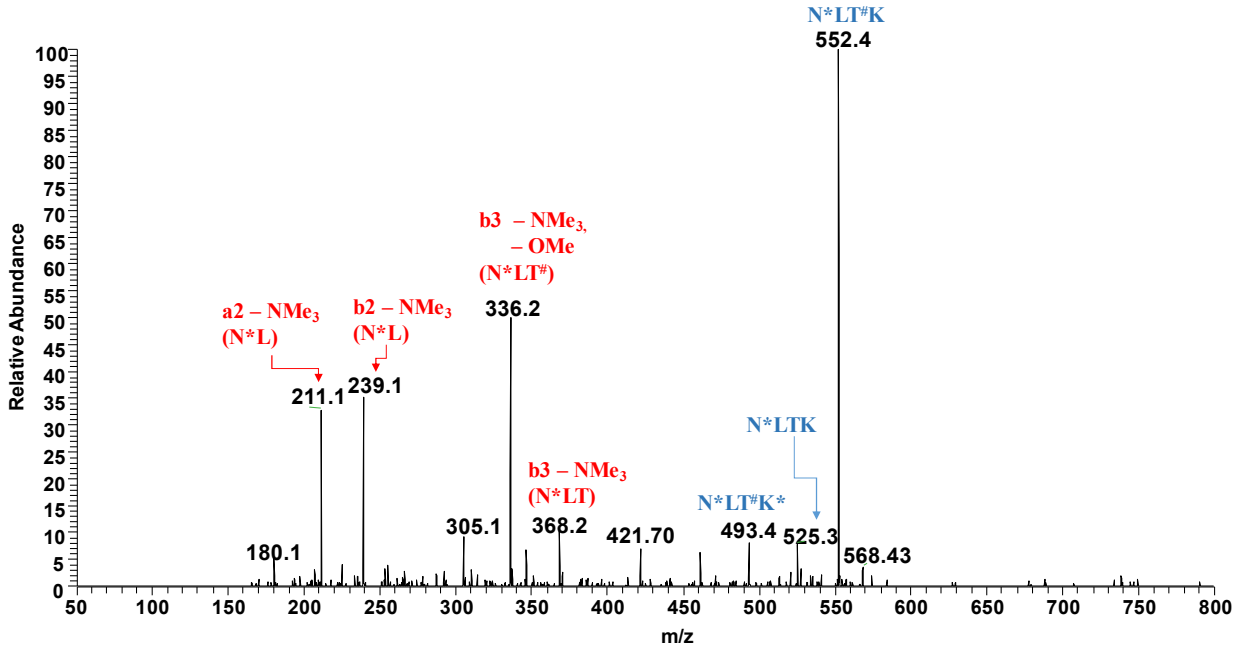

Supp. Figure S10: CID MS^3 fragmentation spectra of peptide N*LTK (generated from the MS^2 of RNase B glycopeptide) at m/z 584.40 (1^+)

Supp. Table S4: N*LTK (From Glycopeptide)

Predicted fragment structure	Amino acid sequence	Fragment type
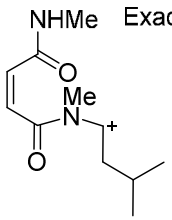 Exact Mass: 211.1441	N*L	a2 - NMe_3
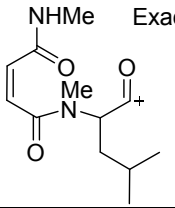 Exact Mass: 239.1390	N*L	b2 - NMe_3
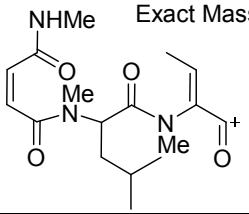 Exact Mass: 336.1918	N*LT	b3 - OMe, - NMe_3

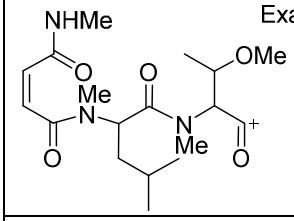 Exact Mass: 368.2180	N*LT	b3 - NMe_3
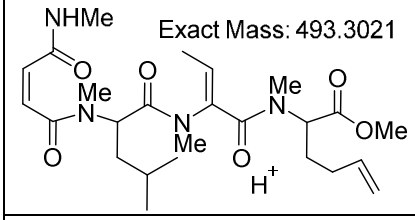 Exact Mass: 493.3021	N*LT$^{\#}$K*	
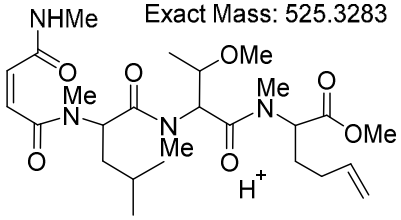 Exact Mass: 525.3283	N*LT*	
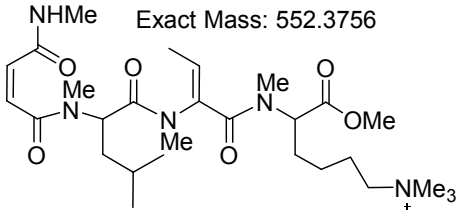 Exact Mass: 552.3756	N*LT$^{\#}$K	
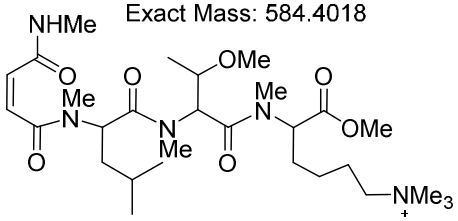 Exact Mass: 584.4018	N*LTK	
* loss of NMe_3 $^{\#}$ loss of OMe		

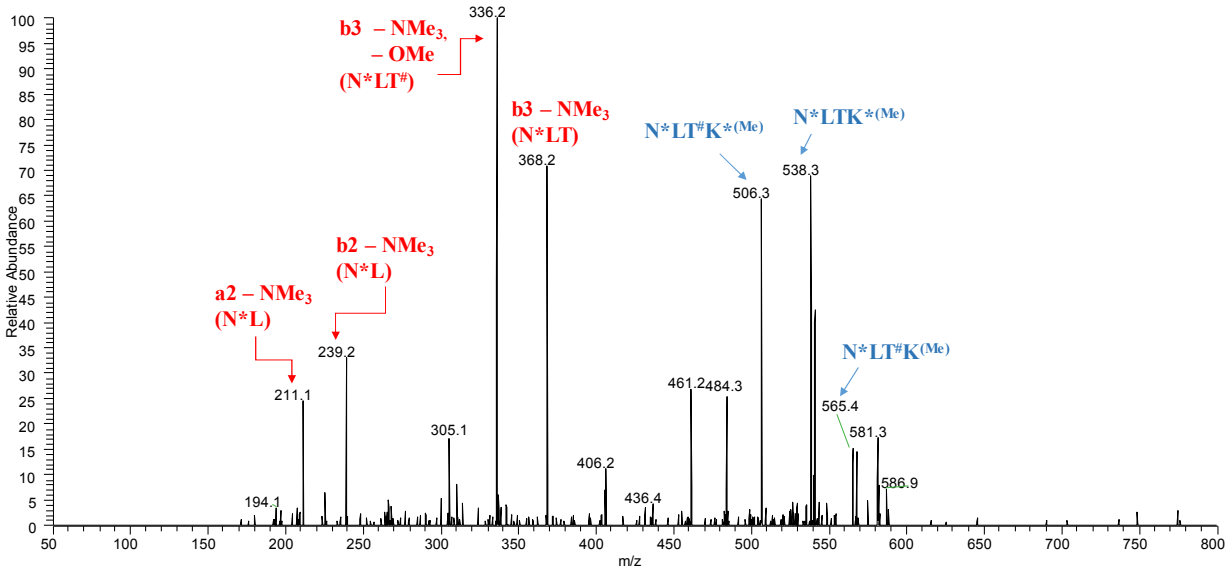

Supp. Figure S11: CID MS^3 fragmentation spectra of peptide $N^*LTK^{(Me)}$ (generated from the MS^2 of RNase B glycopeptide) at m/z 597.43 (1^+)

Supp. Table S5: **$N^*LTK^{(Me)}$ (From Glycopeptide)**

Predicted fragment structure	Amino acid sequence	Fragment type
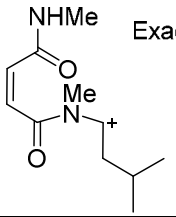 Exact Mass: 211.1441	N*L	a2 - NMe_3
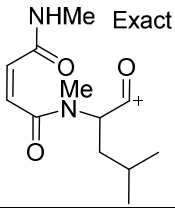 Exact Mass: 239.1390	N*L	b2 - NMe_3
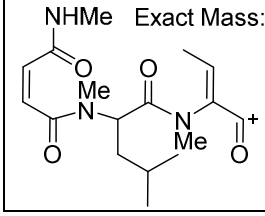 Exact Mass: 336.1918	N*LT#	b3 - OMe, - NMe_3

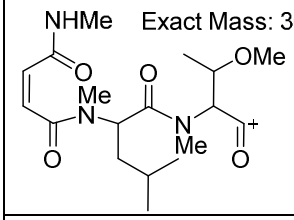	N*LT	b3 - NMe_3
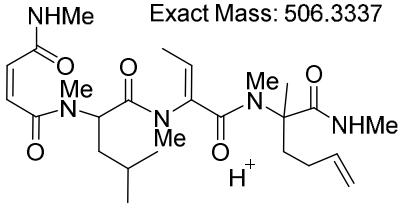	$N*LT^{\#}K*^{(Me)}$	
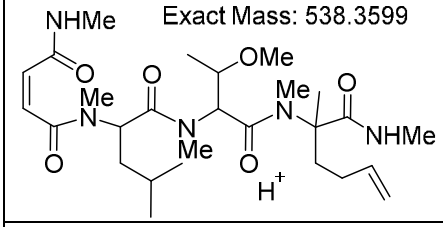	$N*LTK*^{(Me)}$	
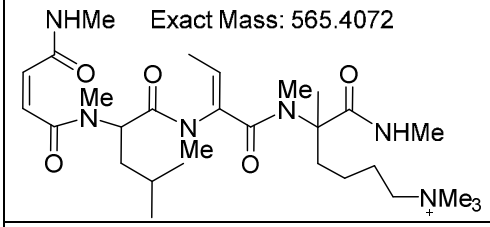	$N*LT^{\#}K^{(Me)}$	
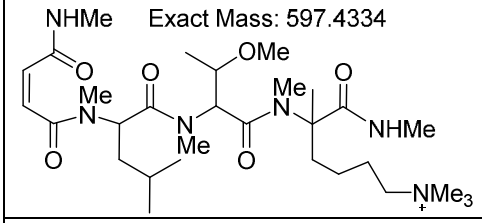	$N*LTK^{(Me)}$	
* loss of NMe_3 # loss of OMe		

Synthetic peptides

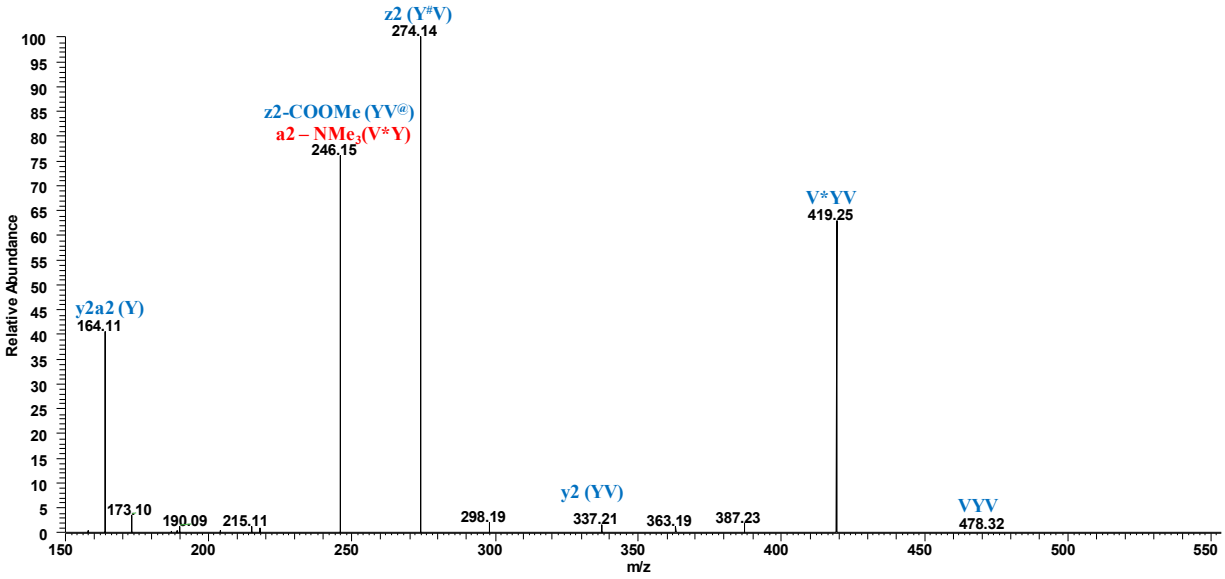

Supp. Figure S12: CID MS^2 fragmentation spectra of peptide VYV at m/z 478.32 (1^+)

Supp. Table S6: VYV

Predicted fragment structure	Amino acid sequence	Fragment type
Exact Mass: 164.1070 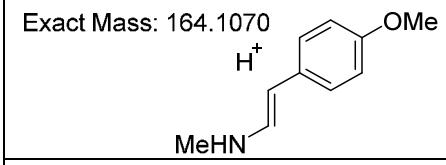	Y	y2a2
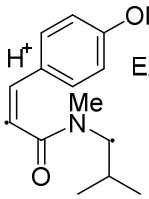 Exact Mass: 246.1489 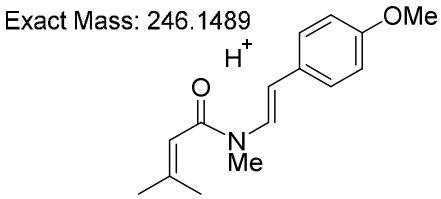	YV@ V*Y	z2 – COOMe a2 - NMe_3
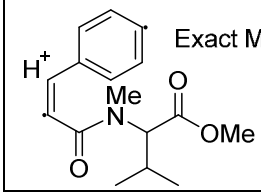 Exact Mass: 274.1438	Y#V	z2 - OMe

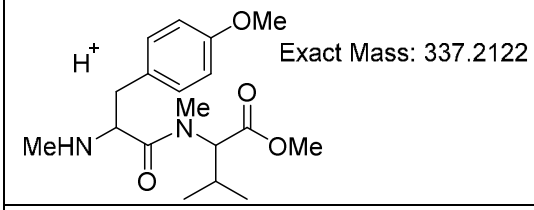	YV	y2
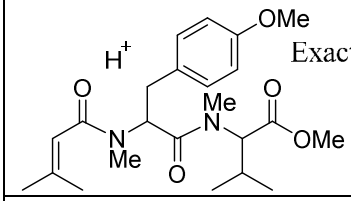	V*YV	
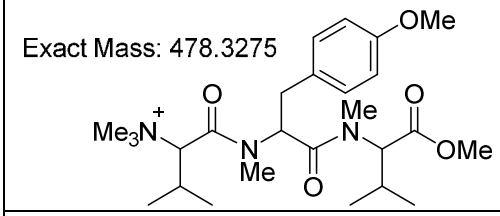	VYV	
* loss of NMe_3 # loss of OMe @ loss of COOMe		

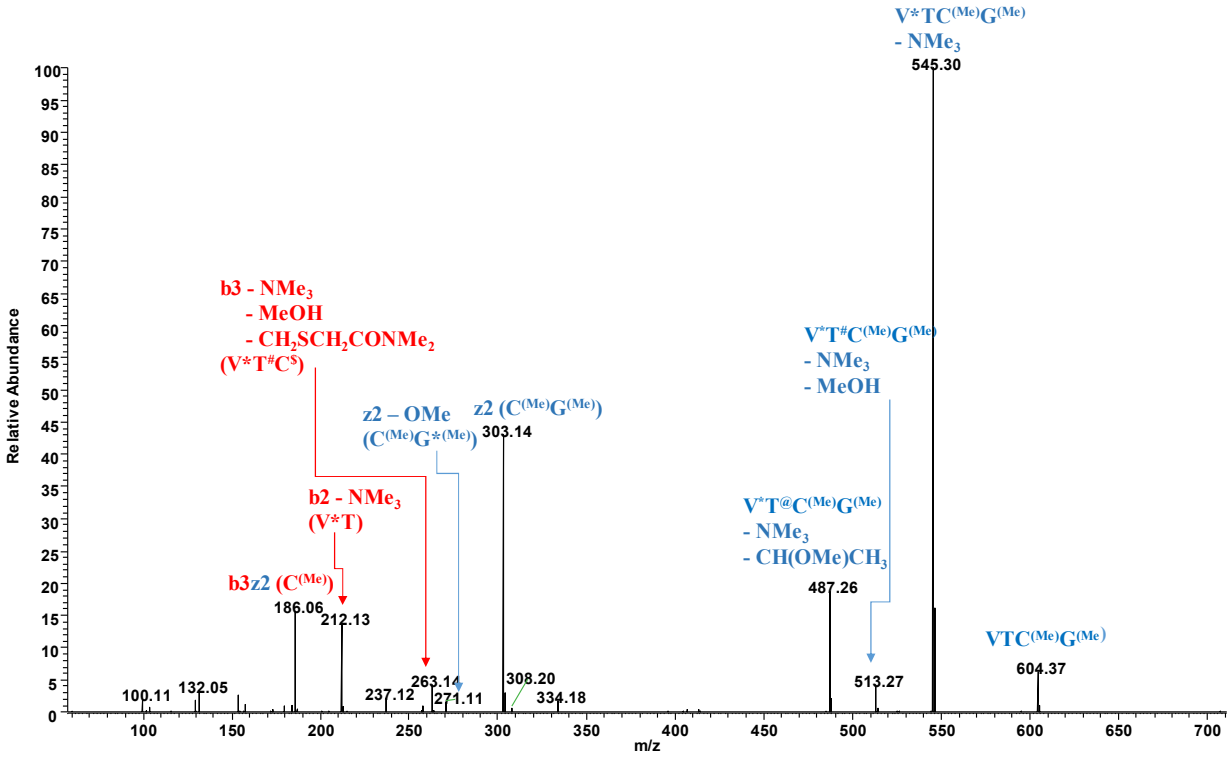

Supp. Figure S13: HCD MS^2 fragmentation spectra of peptide $VTC^{(Me)}G^{(Me)}$ at m/z 604.37 (1^+)

Supp. Table S7: VTC$^{(Me)}$G$^{(Me)}$

Predicted fragment structure	Amino acid sequence	Fragment type
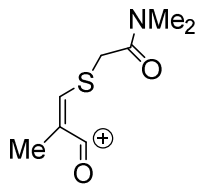 Exact Mass: 186.0583	C$^{(Me)}$	b3z2
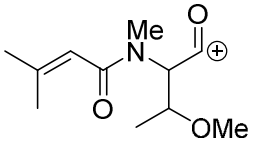 Exact Mass: 212.1281	V*T - NMe_3	b2 - NMe_3
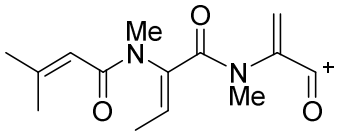 Exact Mass: 263.1390	V*T$^{\#}$C$^{\$}$ - NMe_3 - MeOH - $CH_2SCH_2CONMe_2$	b3 - NMe_3 - MeOH - CH_2SCH_2- $CONMe_2$
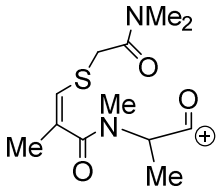 Exact Mass: 271.1111	C$^{(Me)}$G*$^{(Me)}$ - OMe	z2 - OMe
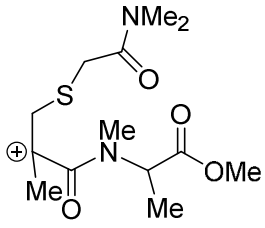 Exact Mass: 303.1373	C$^{(Me)}$G$^{(Me)}$	z2

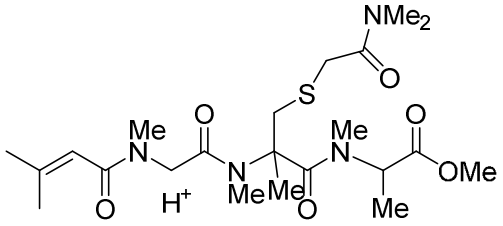 Exact Mass: 487.2585	$V^{*}T^{@}C^{(Me)}G^{(Me)\backslash}$ - NMe_3 - $CH(OMe)CH_3$	
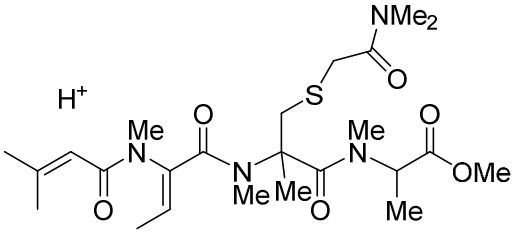 Exact Mass: 513.2741	$V^{*}T^{\#}C^{(Me)}G^{(Me)}$ - NMe_3 - MeOH	
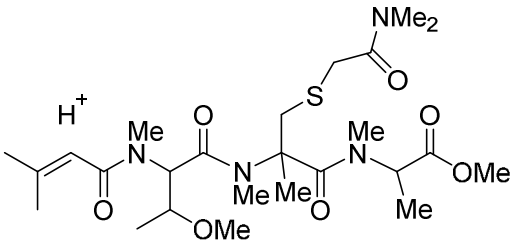 Exact Mass: 545.3003	$V^{*}TC^{(Me)}G^{(Me)}$ - NMe_3	
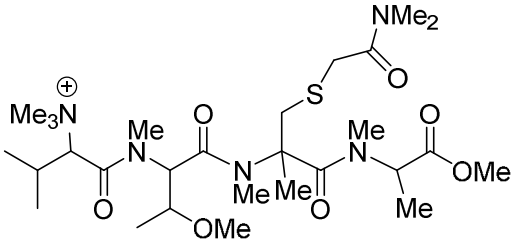 Exact Mass: 604.3738	$VTC^{(Me)}G^{(Me)}$	
* loss of NMe_3 # loss of OMe @ loss of side chain (-CH(OMe)-CH_3) $ loss of side chain (-CH_2-S-CH_2-CO-NMe_2)		

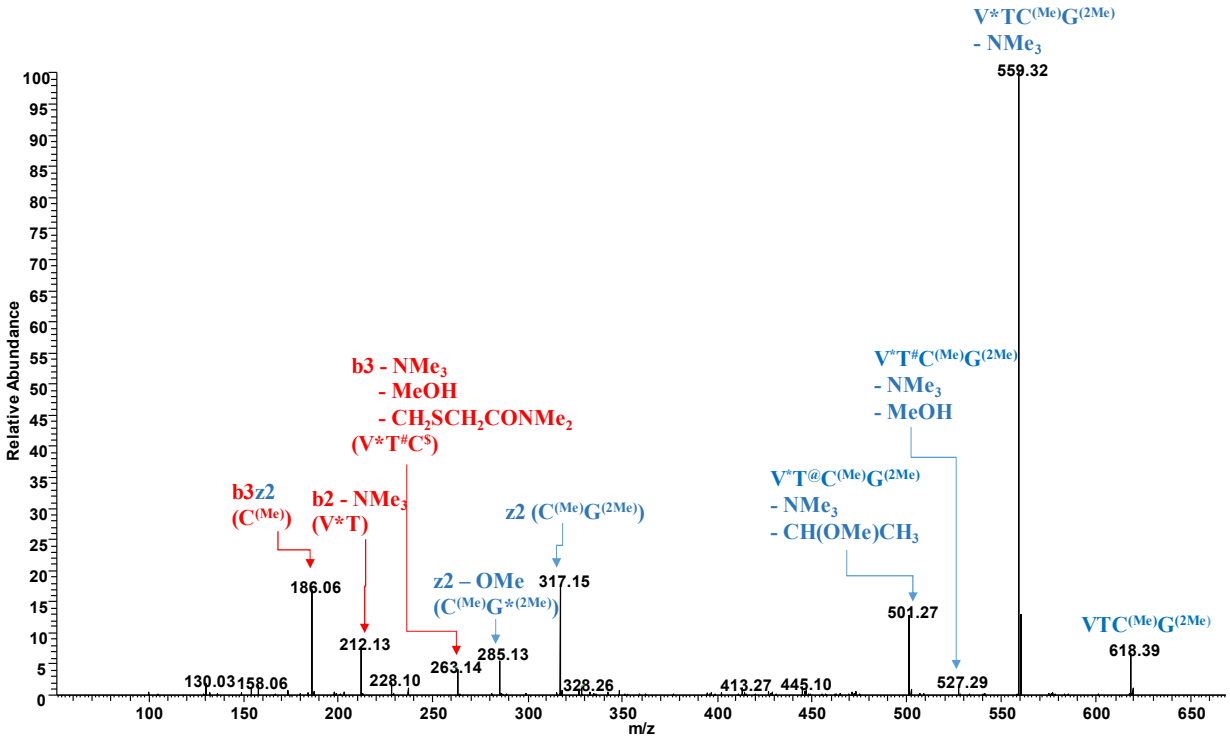

Supp. Figure S14: HCD MS^2 fragmentation spectra of peptide $VTC^{(Me)}G^{(2Me)}$ at m/z 618.39 (1^+)

Supp. Table S8: $VTC^{(Me)}G^{(2Me)}$

Predicted fragment structure	Amino acid sequence	Fragment type
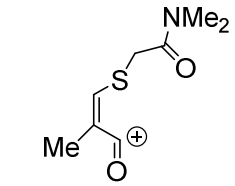 Exact Mass: 186.0583	$C^{(Me)}$	b3z2
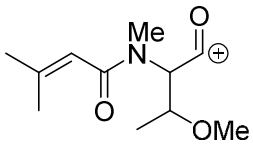 Exact Mass: 212.1281	V*T	b2

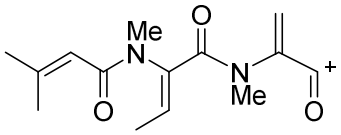 Exact Mass: 263.1390	$V^{*}T^{\#}C^{\$}$ - NMe_3 - MeOH - $CH_2SCH_2CONMe_2$	b3 - NMe_3 - MeOH - CH_2SCH_2- $CONMe_2$
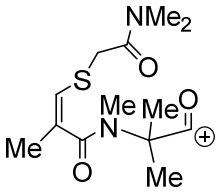 Exact Mass: 285.1267	$C^{(Me)}G^{*(Me_2)}$ - OMe	z2 - OMe
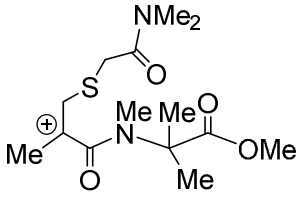 Exact Mass: 318.1613	$C^{(Me)}G^{(Me_2)}$	z2
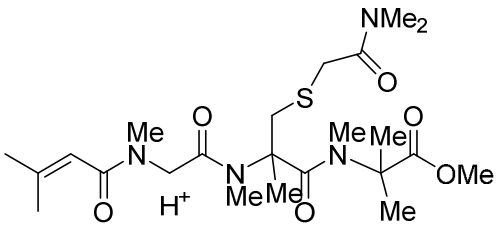 Exact Mass: 501.2741	$V^{*}T^{@}C^{(Me)}G^{(Me_2)}$ - NMe_3 - $CH(OMe)CH_3$	
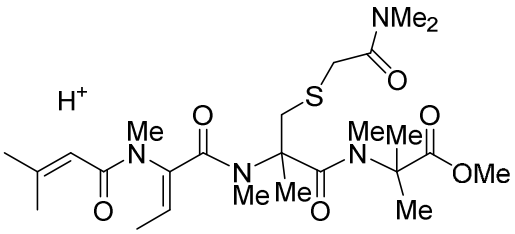 Exact Mass: 527.2898	$V^{*}T^{\#}C^{(Me)}G^{(Me_2)}$ - NMe_3 - MeOH	

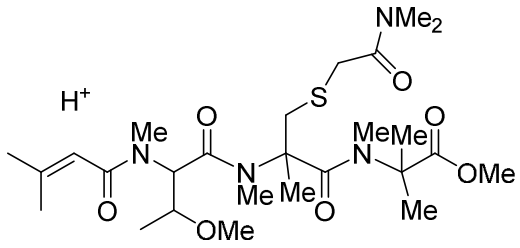 Exact Mass: 559.3160	$V^{*}TC^{(Me)}G^{(Me_2)}$ - NMe_3	
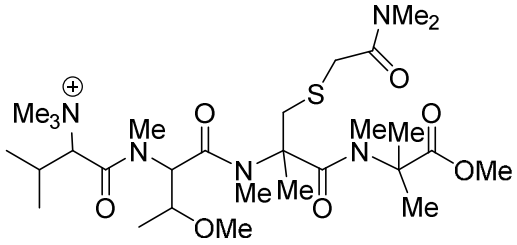 Exact Mass: 618.3895	$VTC^{(Me)}G^{(Me_2)}$	
* loss of NMe_3 # loss of OMe @ loss of side chain (-CH(OMe)-CH_3) $ loss of side chain (-CH_2-S-CH_2-CO-NMe_2)		

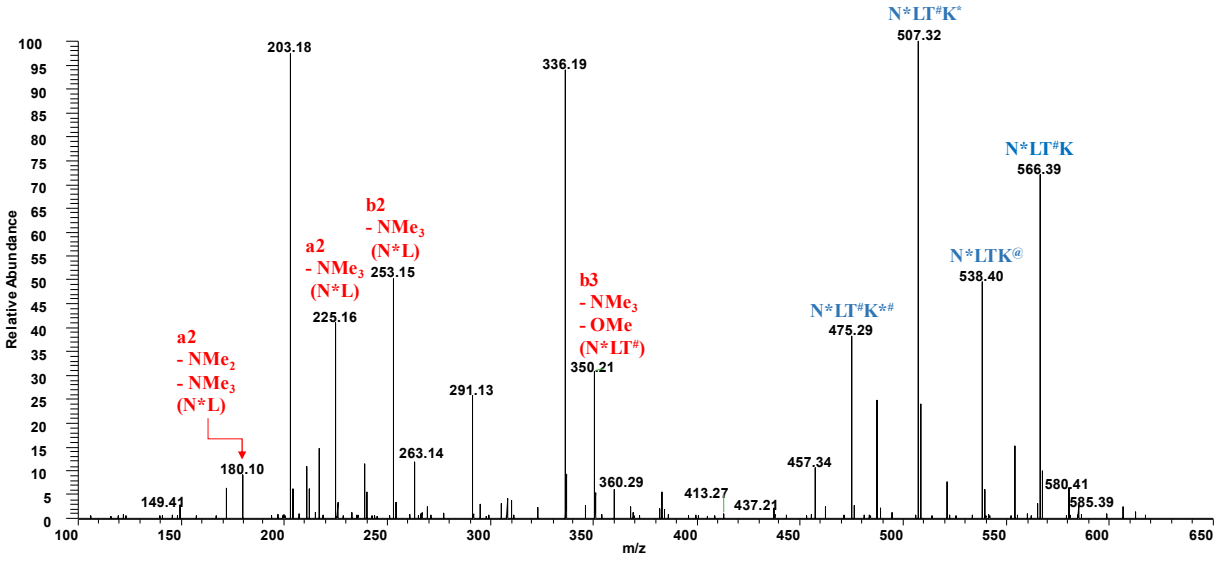

Supp. Figure S15: CID MS^2 fragmentation spectra of peptide N*LTK at m/z 598.44 (1^+)

Supp. Table S9: N*LTK (synthetic peptide)

Predicted fragment structure	Amino acid sequence	Fragment type
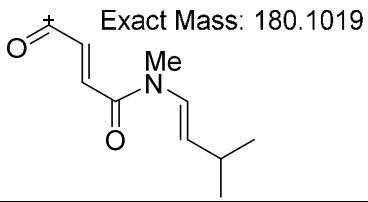 Exact Mass: 180.1019	N*L	a2 - NMe_3 - NMe_2
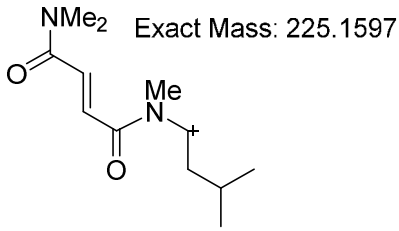 Exact Mass: 225.1597	N*L	a2 - NMe_3
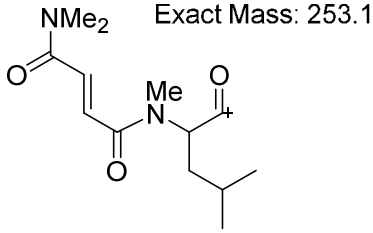 Exact Mass: 253.1546	N*L	b2 - NMe_3
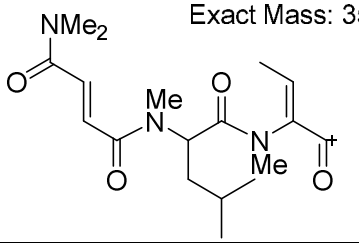 Exact Mass: 350.2074	N*LT#	b3 - NMe_3 - OMe
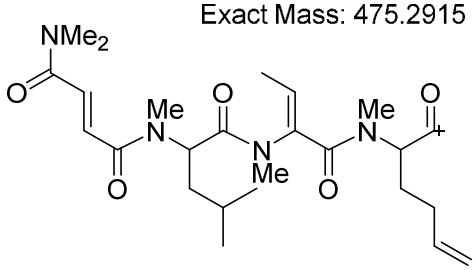 Exact Mass: 475.2915	N*LT#K*#	

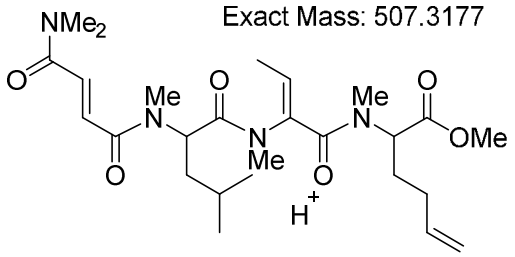 Exact Mass: 507.3177	N*LT#K*	
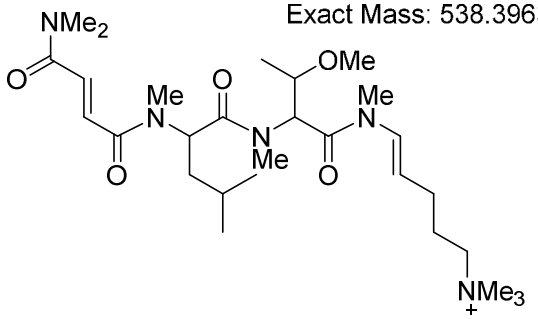 Exact Mass: 538.3963	N*LTK@	
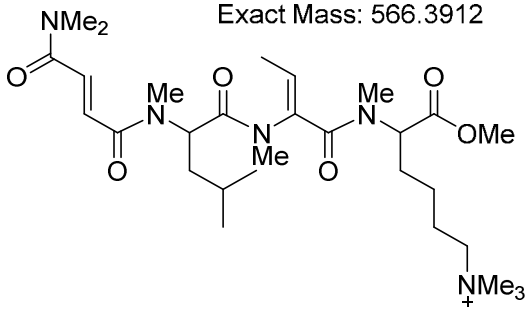 Exact Mass: 566.3912	N*LT#K	
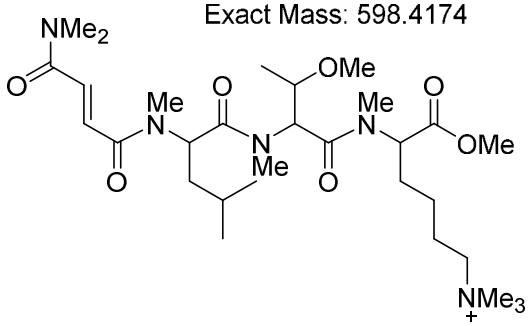 Exact Mass: 598.4174	N*LTK	
* loss of NMe_3 # loss of OMe @ loss of COOMe		

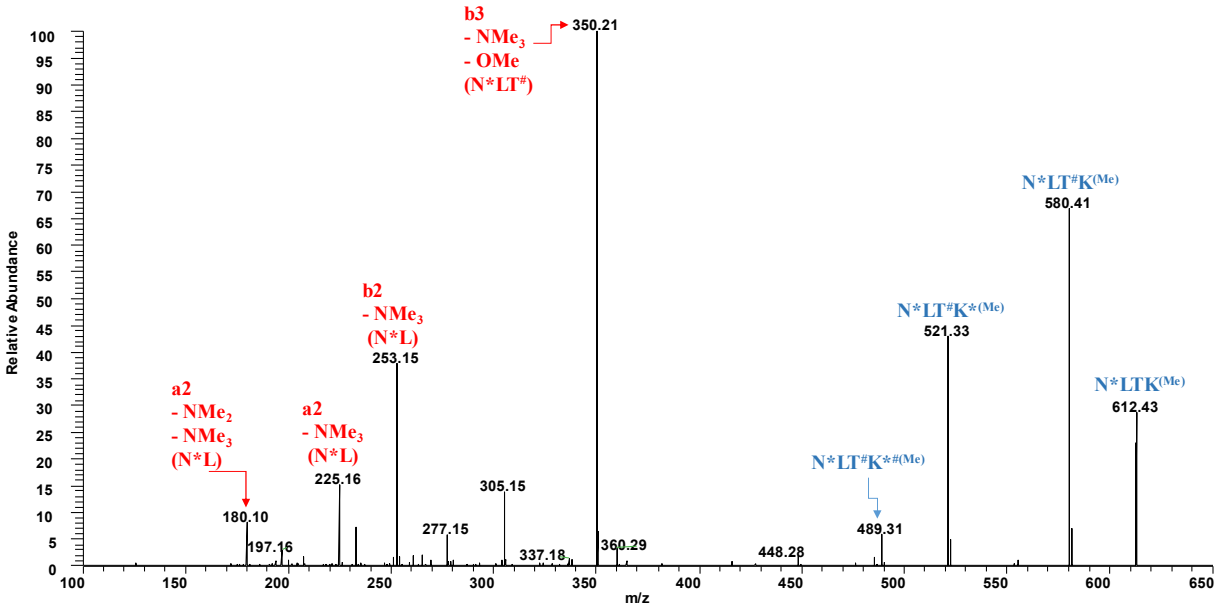

Supp. Figure S16: CID MS^3 fragmentation spectra of peptide $N^*LTK^{(Me)}$ at m/z 612.43 (1^+)

Supp. Table S10: $N^*LTK^{(Me)}$ (synthetic peptide)

Predicted fragment structure	Amino acid sequence	Fragment type
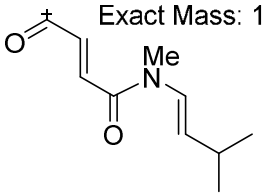	N*L	a2 - NMe_3 - NMe_2
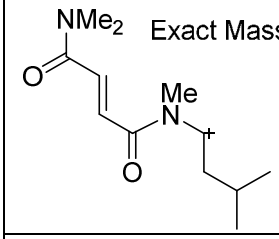	N*L	a2 - NMe_3
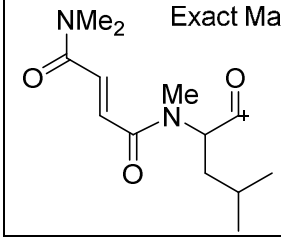	N*L	b2 - NMe_3

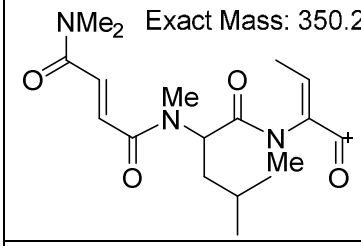 Exact Mass: 350.2074	N*LT$^{\#}$	b3 - NMe_3 - OMe
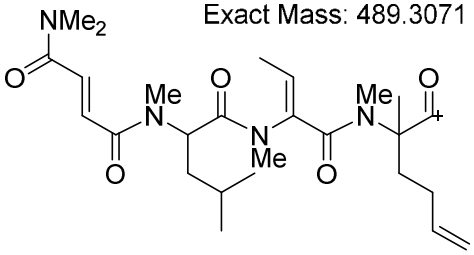 Exact Mass: 489.3071	N*LT$^{\#}$K*$^{\#(Me)}$	
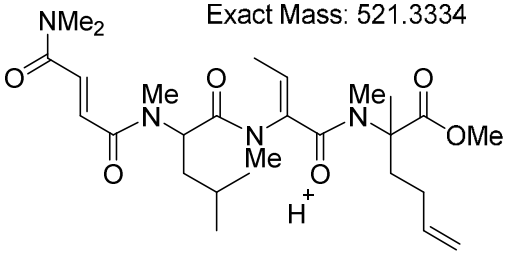 Exact Mass: 521.3334	N*LT$^{\#}$K*$^{(Me)}$	
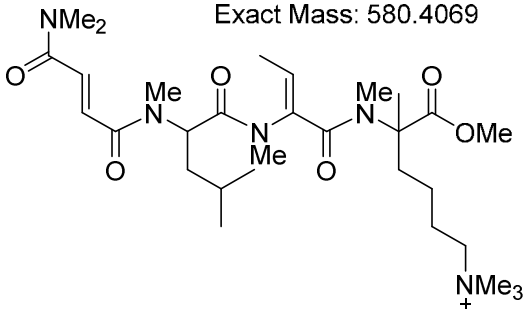 Exact Mass: 580.4069	N*LT$^{\#}$K$^{(Me)}$	
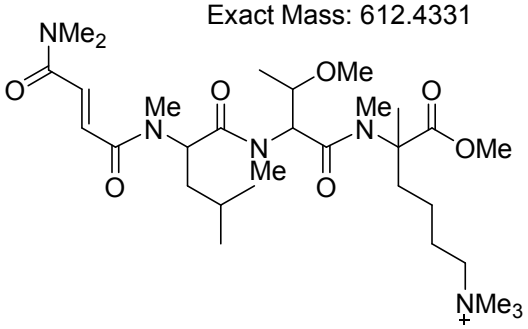 Exact Mass: 612.4331	N*LTK$^{(Me)}$	
* loss of NMe_3 # loss of OMe		

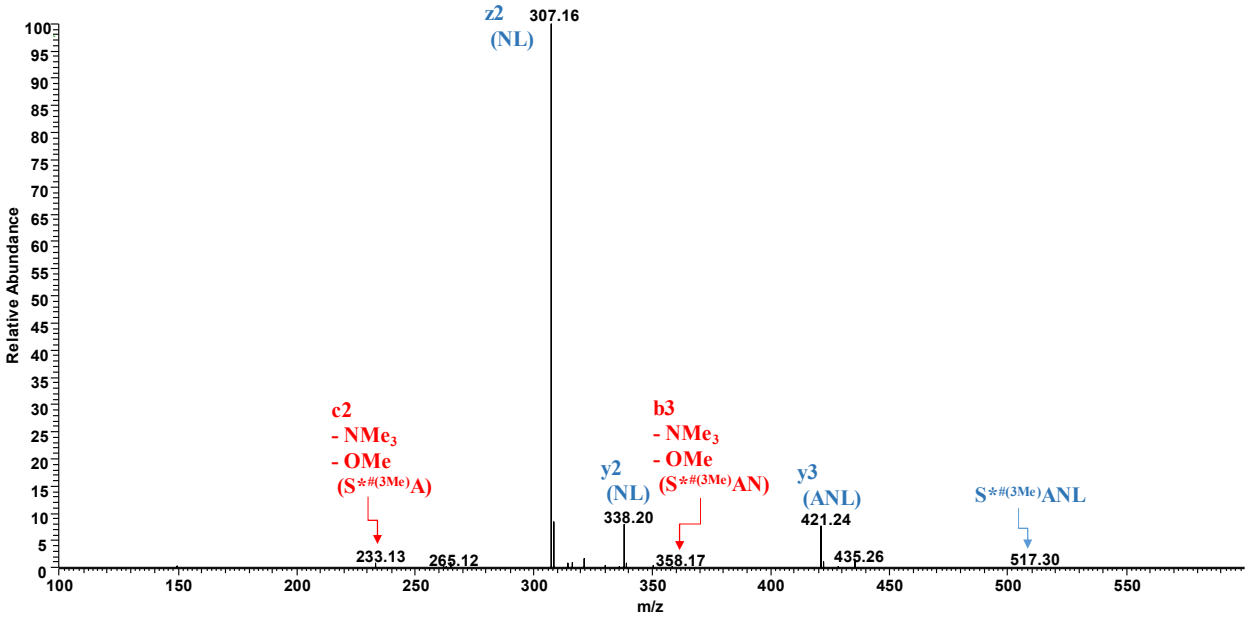

Supp. Figure S17: CID MS^2 fragmentation spectra of peptide $S^{*\#(3Me)}ANL$ at m/z 517.30 (1^+)

Supp. Table S11: $S^{*\#(3Me)}ANL$ (synthetic peptide)

Predicted fragment structure	Amino acid sequence	Fragment type
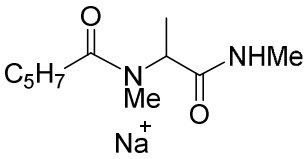 Exact Mass: 233.1260	$S^{*\#(3Me)}A$	c2 - NMe_3 - OMe
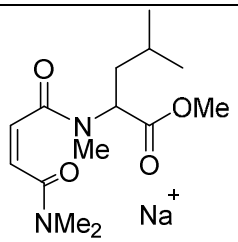 Exact Mass: 307.1628	NL	z2
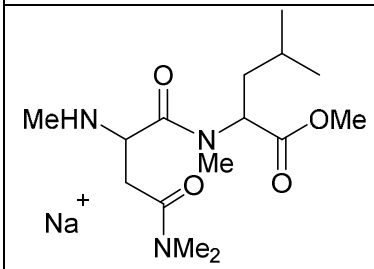 Exact Mass: 338.2050	NL	y2

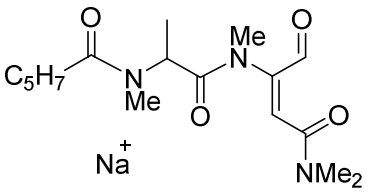 Exact Mass: 358.1737	$S^{*\#(3Me)}AN$	b3 - NMe_3 - OMe
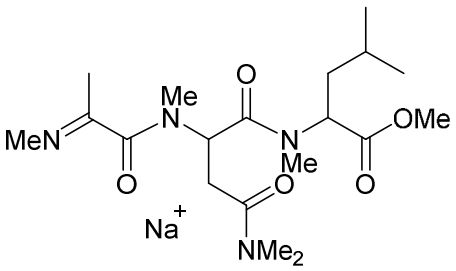 Exact Mass: 421.2421	ANL	y3
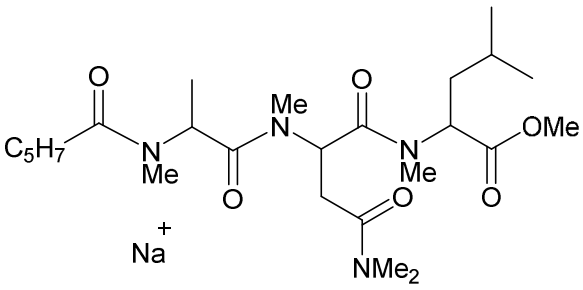 Exact Mass: 517.2997	$S^{*\#(3Me)}ANL$	
* loss of NMe_3 # loss of OMe		

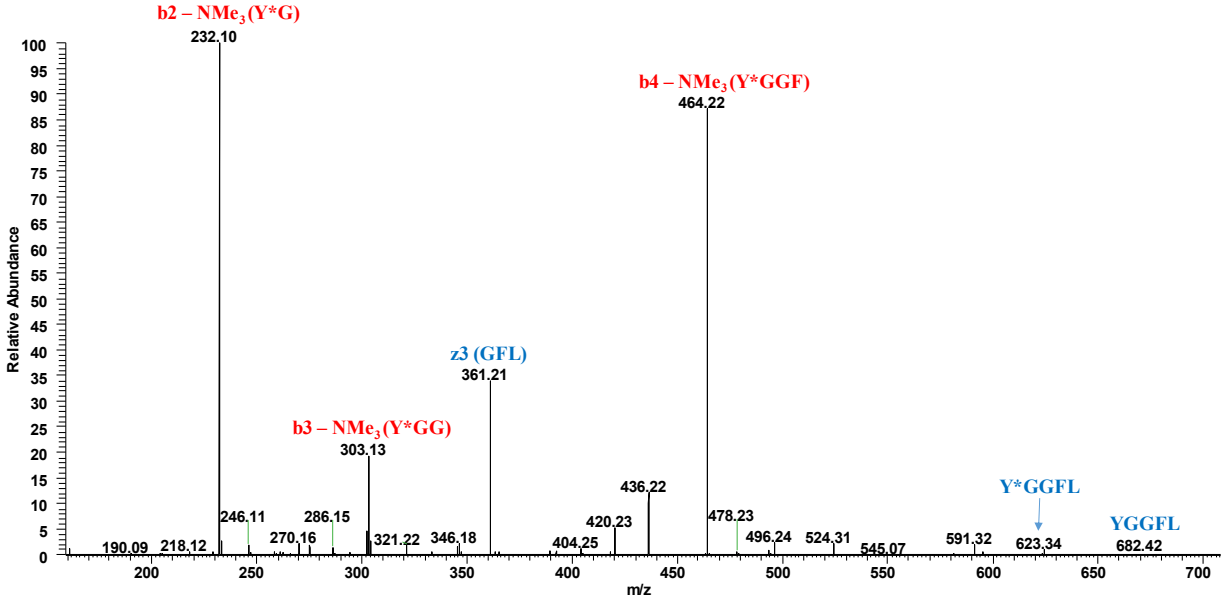

Supp. Figure S18: CID MS^2 fragmentation spectra of peptide YGGFL at m/z 682.42 (1^+)

Supp. Table S12: YGGFL

Predicted fragment structure	Amino acid sequence	Fragment type
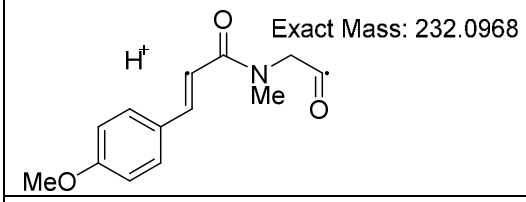	Y*G	b2 - NMe_3
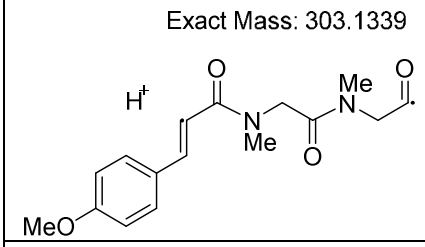	Y*GG	b3 - NMe_3
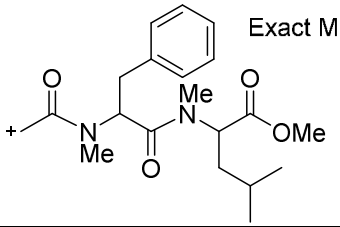	GFL	z3
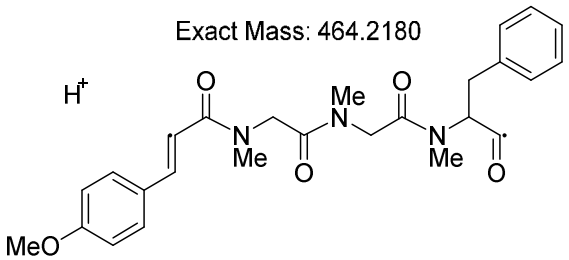	Y*GGF	b4 - NMe_3
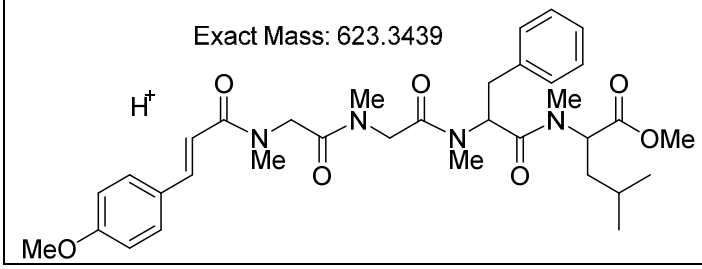	Y*GGFL	

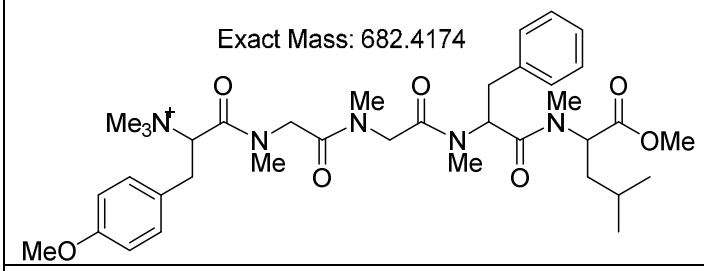	YGGFL	
* loss of NMe_3		

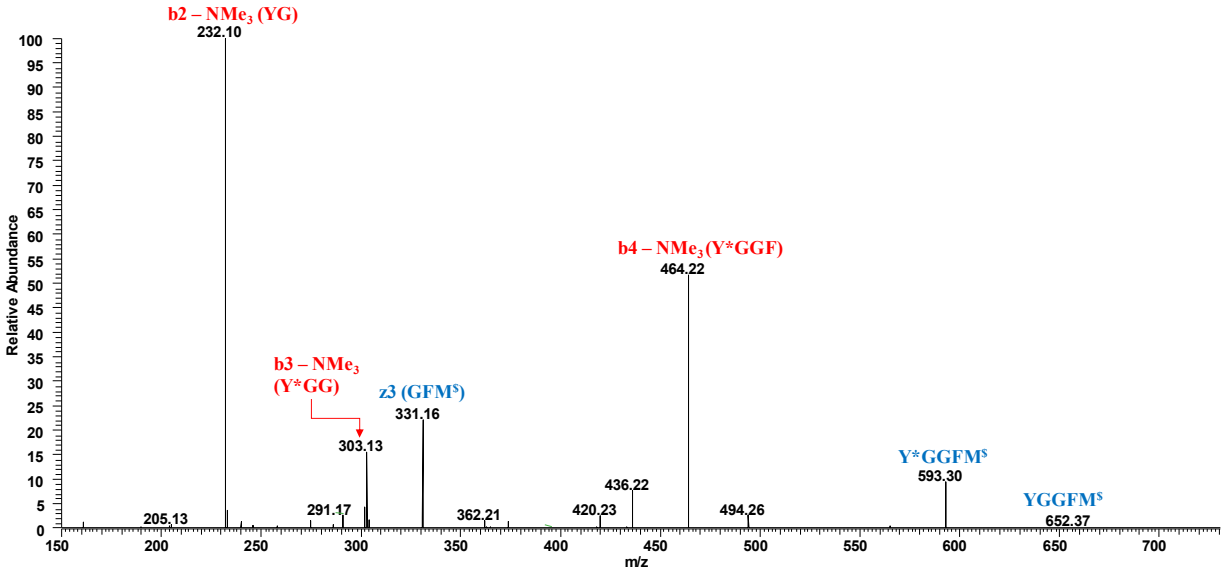

Supp. Figure S19: CID MS^2 fragmentation spectra of peptide $YGGFM^{\$}$ at m/z 652.37 (1^+)

Supp. Table S13: $YGGFM^{\$}$

Predicted fragment structure	Amino acid sequence	Fragment type
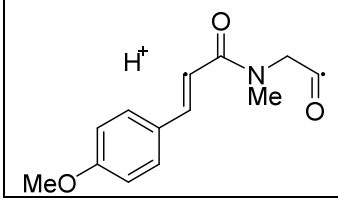	Y*G	b2 - NMe_3

Exact Mass: 303.1339 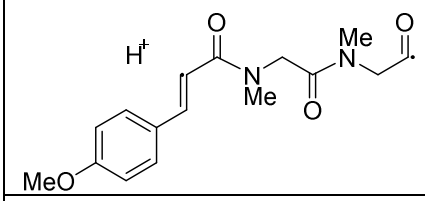	Y*GG	b3 - NMe_3
Exact Mass: 331.1652 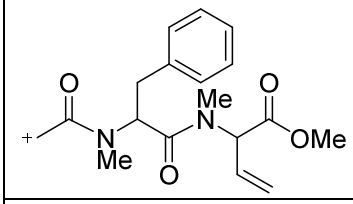	GFM$	z3 - SMe
Exact Mass: 464.2180 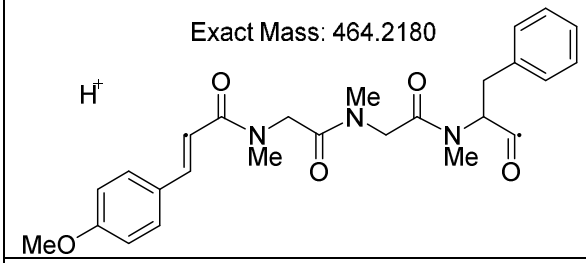	Y*GGF	b4 - NMe_3
Exact Mass: 593.2970 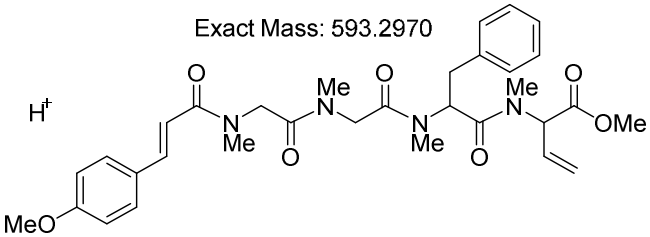	Y*GGFM$	
Exact Mass: 652.3705 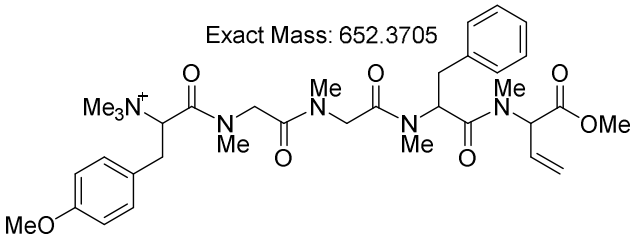	YGGFM$	
* - loss of NMe_3 $ - loss of SMe		

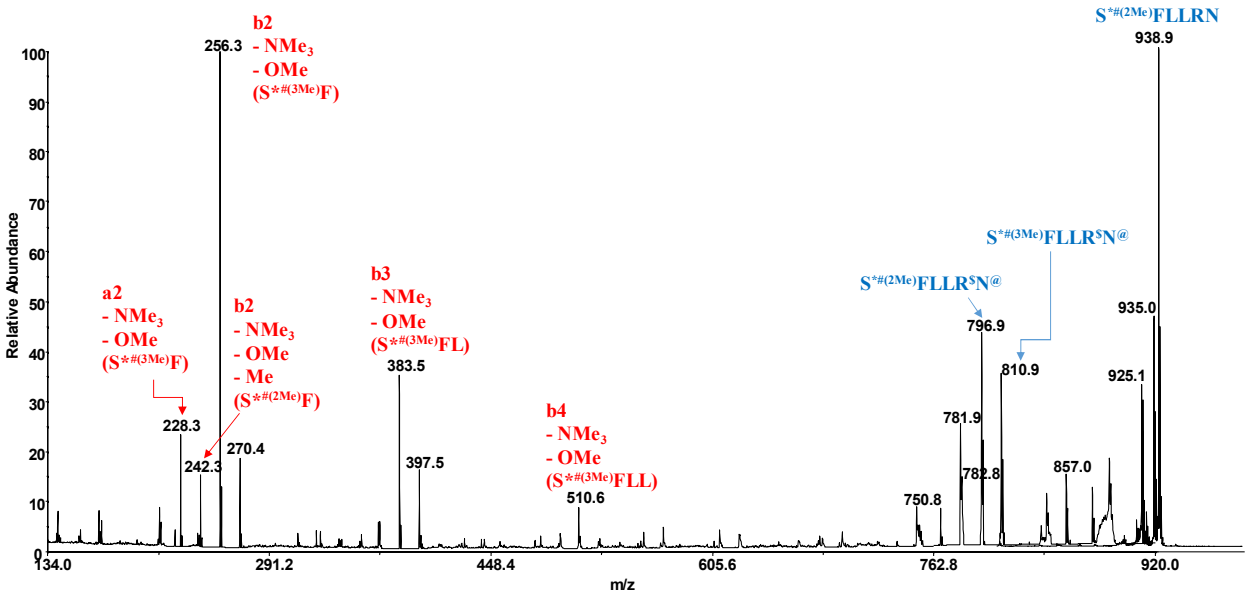

Supp. Figure S20: CID MS^2 fragmentation spectra of peptide $S^{*\#(3Me)}FLLRN$ at m/z 952.65 (1^+)

Supp. Table S14: **S*FLLRN**

Predicted fragment structure	Amino acid sequence	Fragment type
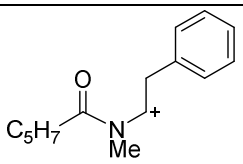 Exact Mass: 228.1383	$S^{*\#(3Me)}F$	a2 - NMe_3 - OMe
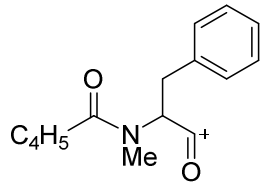 Exact Mass: 242.1176	$S^{*\#(2Me)}F$	b2 - NMe_3 - OMe - Me
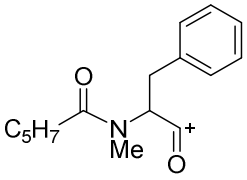 Exact Mass: 256.1332	$S^{*\#(3Me)}F$	b2 - NMe_3 - OMe

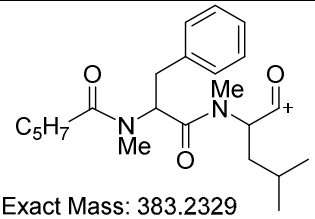 Exact Mass: 383.2329	S*#(3Me)FL	b3 - NMe_3 - OMe
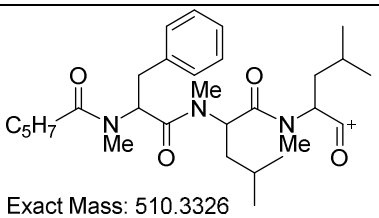 Exact Mass: 510.3326	S*#(3Me)FLL	b4 - NMe_3 - OMe
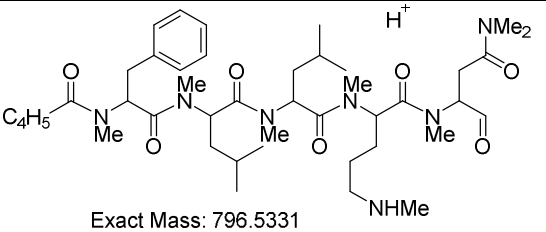 Exact Mass: 796.5331	S*#(2Me)FLLR$N@	
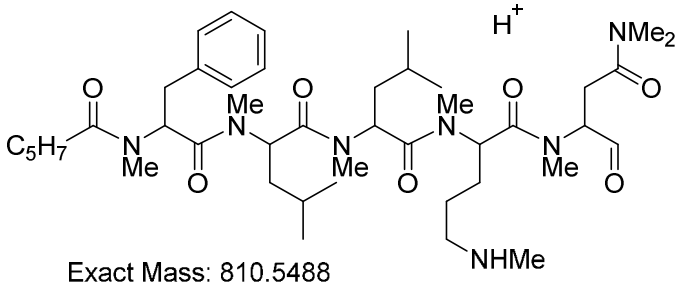 Exact Mass: 810.5488	S*#(3Me)FLLR$N@	
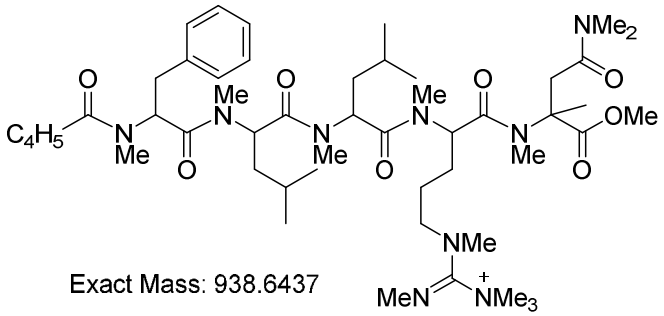 Exact Mass: 938.6437	S*#(2Me)FLLRN	
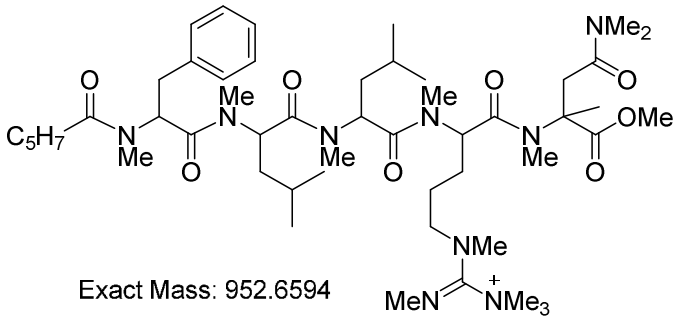 Exact Mass: 952.6594	S*#(3Me)FLLRN	

* - loss of NMe_3 $ - C(NMe)NMe_2 @ - loss of COOMe

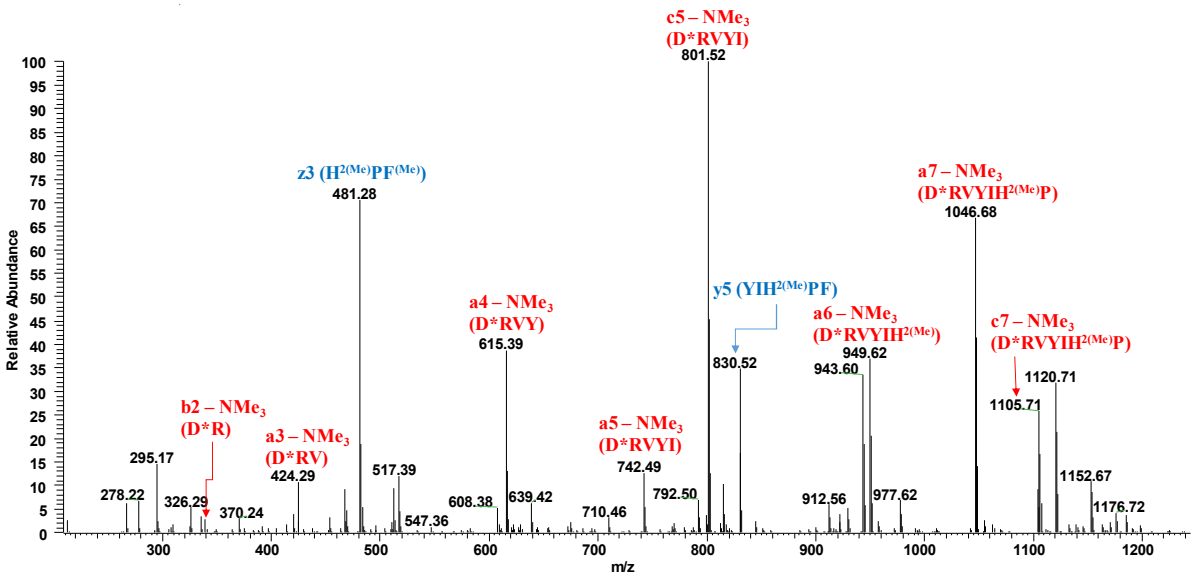

Supp. Figure S21: CID MS^2 fragmentation spectra of peptide D*RVYIHPF at m/z 1281.79 (1^+)

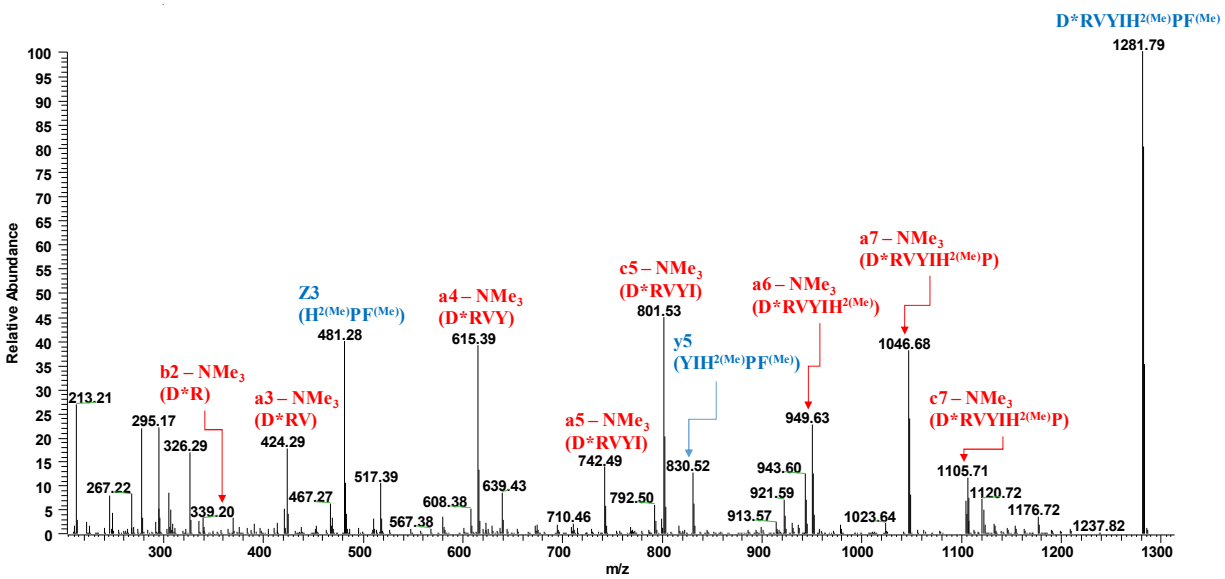

Supp. Figure S22: HCD MS^2 fragmentation spectra of peptide D*RVYIH$^{2(Me)}$PF$^{(Me)}$ at m/z 1281.79 (1^+)

Supp. Table S15: D*RVYIH$^{2(Me)}$PF$^{(Me)}$

Predicted fragment structure	Amino acid sequence	Fragment type
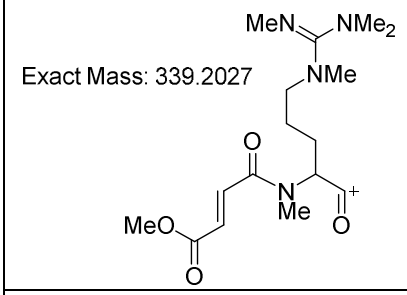	D*R	b2 - NMe_3
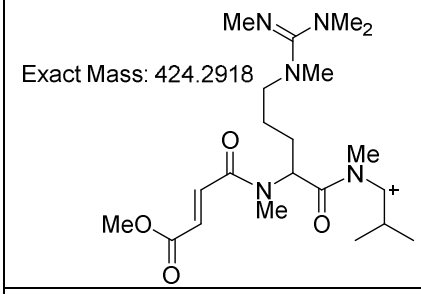	D*RV	a3 - NMe_3
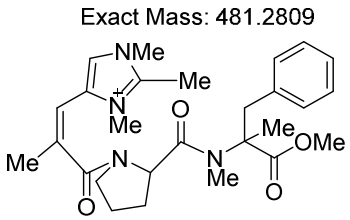	HPF	z3
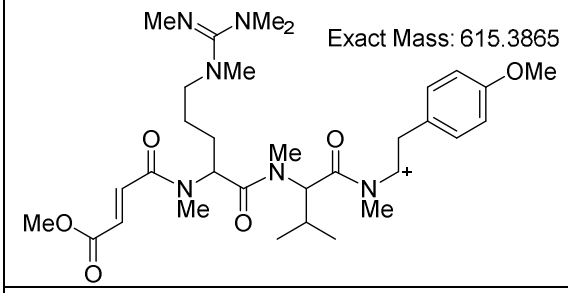	D*RVY	a4 - NMe_3
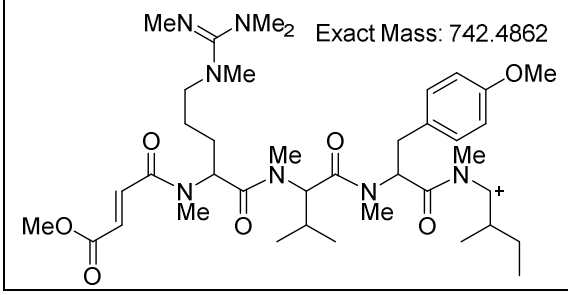	D*RVYI	a5 - NMe_3

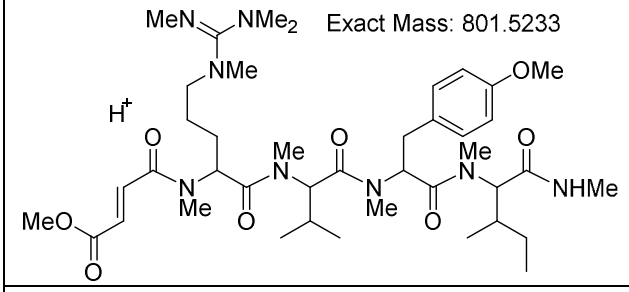 Exact Mass: 801.5233	D*RVYI	c5 - NMe_3
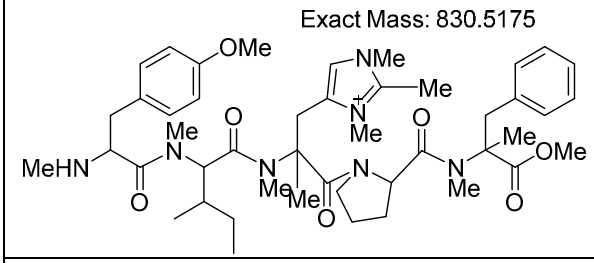 Exact Mass: 830.5175	$YIH^{2(Me)}PF^{(Me)}$	y5
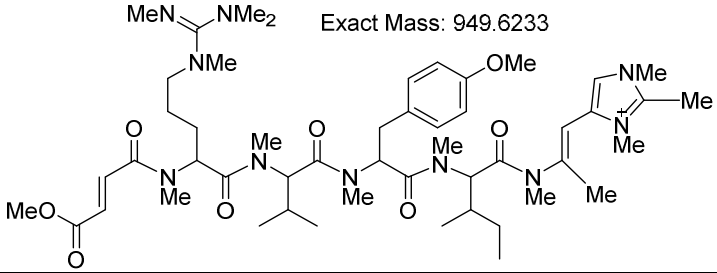 Exact Mass: 949.6233	$D*RVYIH^{2(Me)}$	a6 - NMe_3
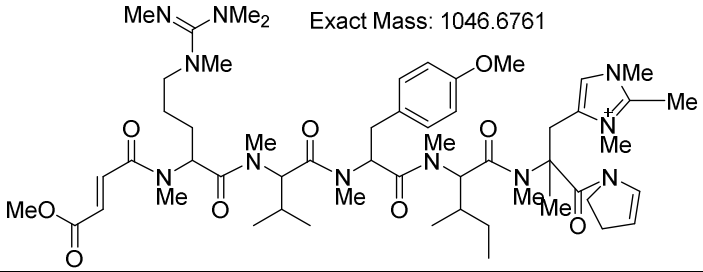 Exact Mass: 1046.6761	$D*RVYIH^{2(Me)}P$	a7 - NMe_3
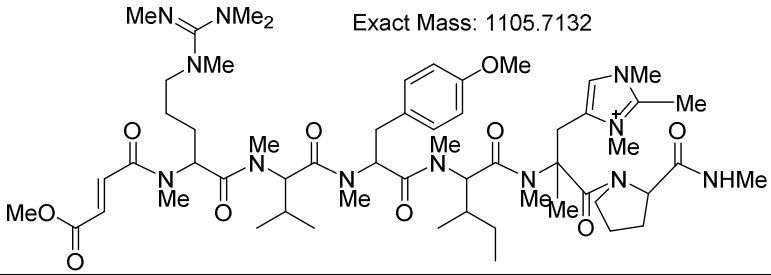 Exact Mass: 1105.7132	$D*RVYIH^{2(Me)}P$	c7 - NMe_3

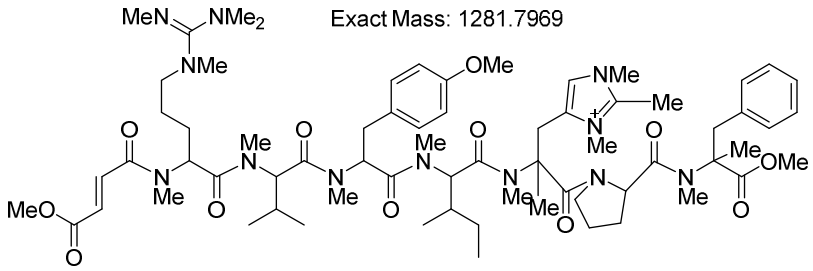	D*RVYIH$^{2(Me)}$PF$^{(Me)}$	
* - loss of NMe_3		

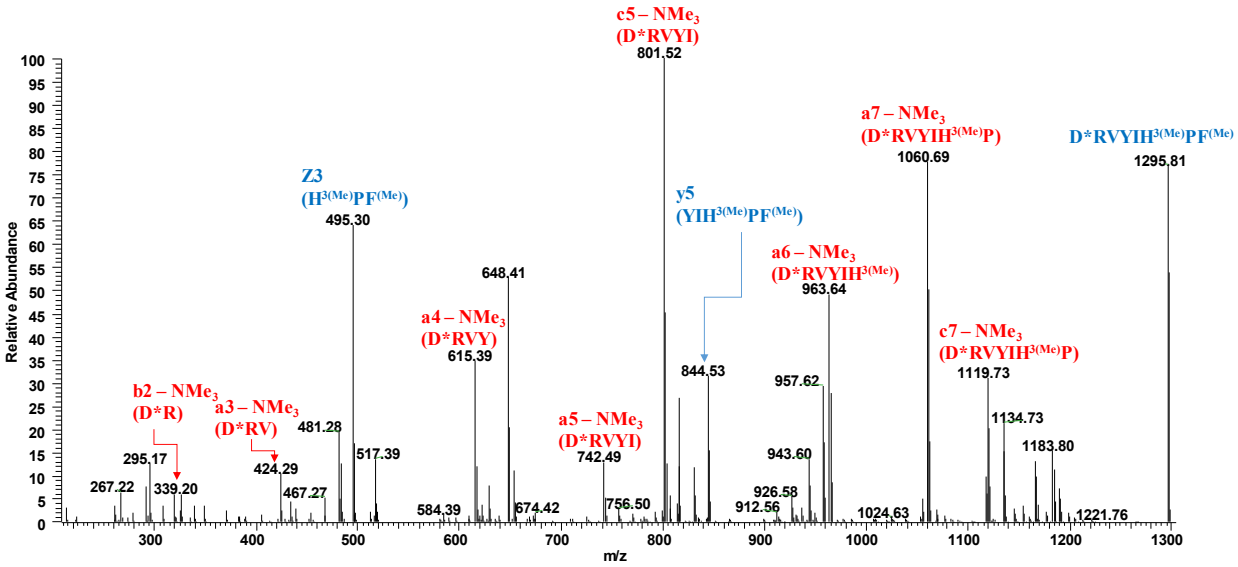

Supp. Figure S23: CID MS^2 fragmentation spectra of peptide D*RVYIH$^{3(Me)}$PF$^{(Me)}$ at m/z 1295.81 (1^+)

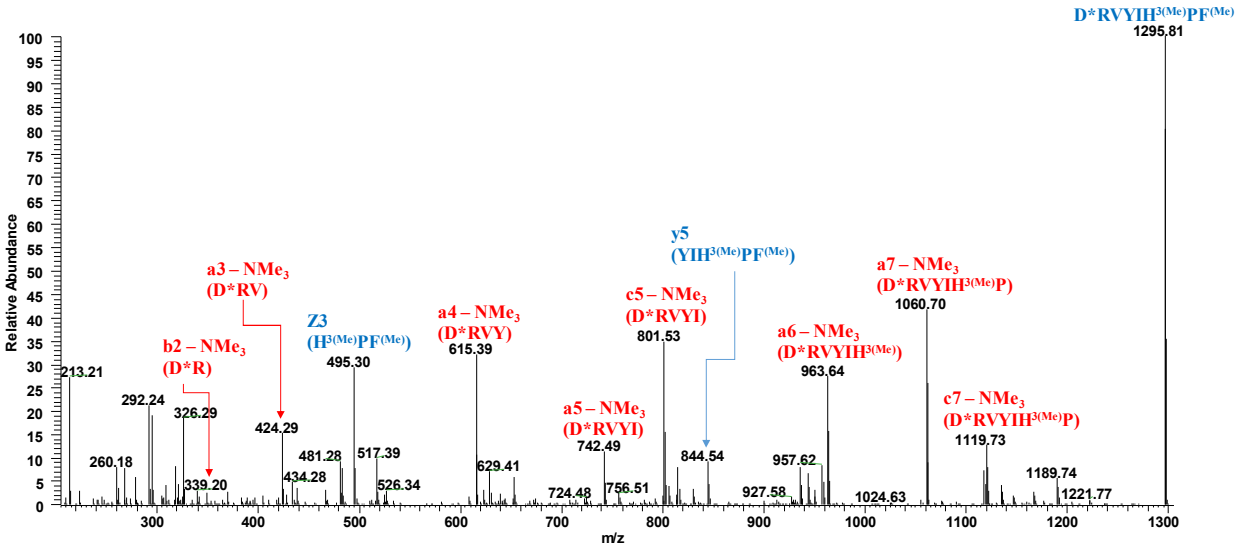

Supp. Figure S24: HCD MS^2 fragmentation spectra of peptide D*RVYIH$^{3(Me)}$PF$^{(Me)}$at m/z 1295.81 (1^+)

Supp. Table S16: **D*RVYIH$^{3(Me)}$PF$^{(Me)}$**

Predicted fragment structure	Amino acid sequence	Fragment type
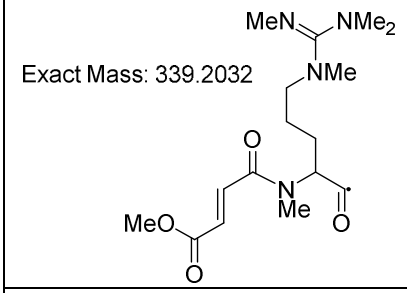	D*R	b2 - NMe_3
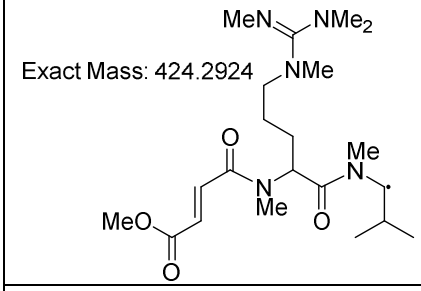	D*RV	a3 - NMe_3
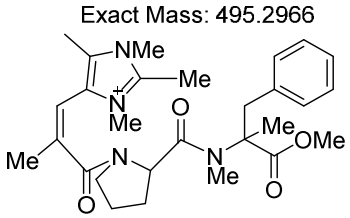	$H^{3(Me)}PF^{(Me)}$	z3
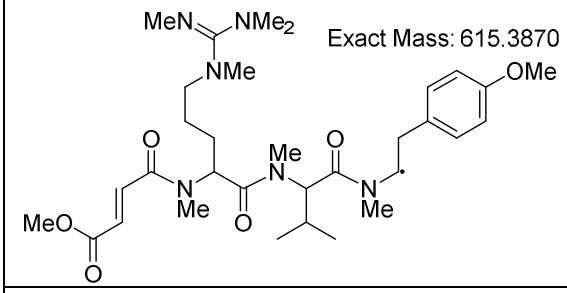	D*RVY	a4 - NMe_3
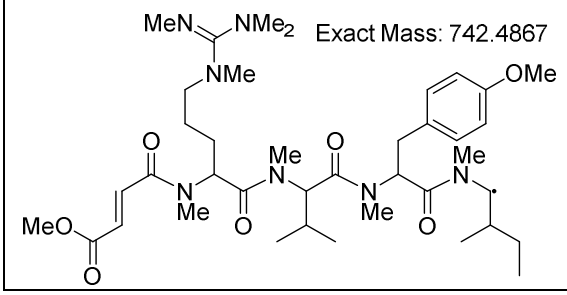	D*RVYI	a5 - NMe_3

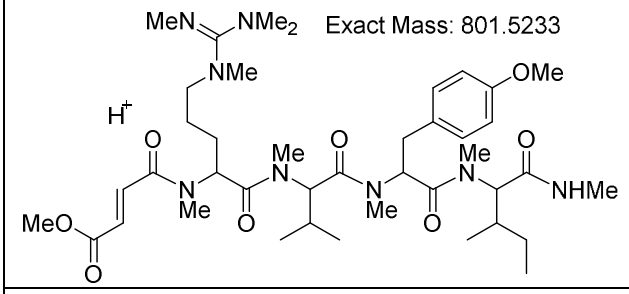 Exact Mass: 801.5233	D*RVYI	c5 - NMe_3
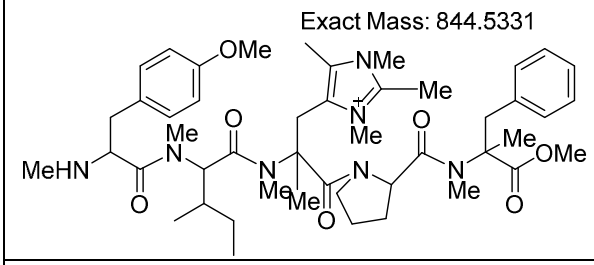 Exact Mass: 844.5331	$YIH^{3(Me)}PF^{(Me)}$	y5
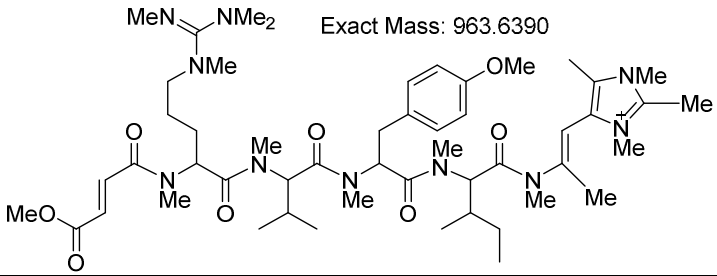 Exact Mass: 963.6390	$D*RVYIH^{3(Me)}$	a6 - NMe_3
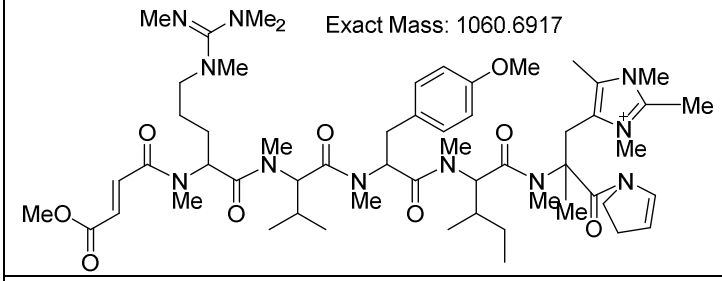 Exact Mass: 1060.6917	$D*RVYIH^{3(Me)}P$	a7 - NMe_3
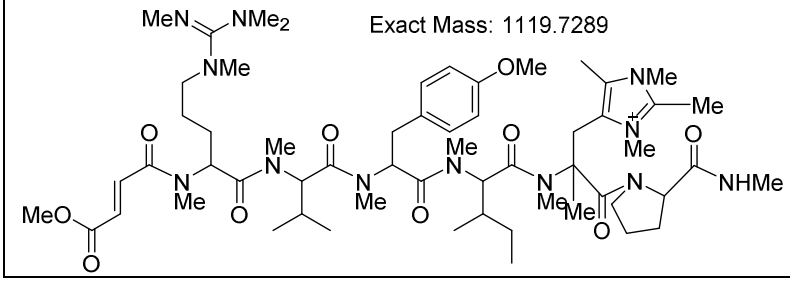 Exact Mass: 1119.7289	$D*RVYIH^{3(Me)}P$	c7 - NMe_3

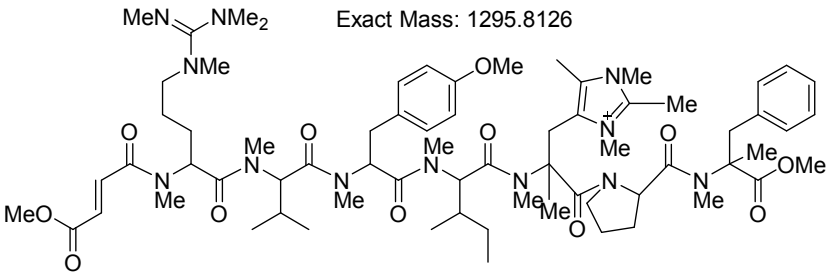	D*RVYIH$^{3(Me)}$P F$^{(Me)}$	
* - loss of NMe_3		

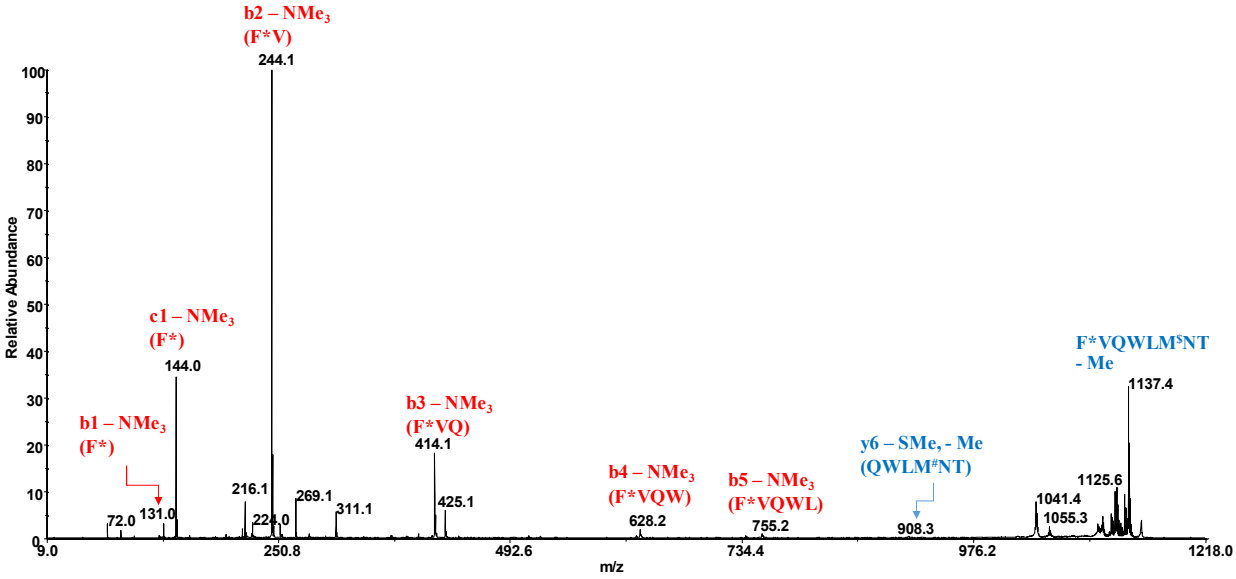

Supp. Figure S25: CID MS^2 fragmentation spectra of peptide F*VQWLM$^{\$}NT^{(Me)}$ at m/z 1151.70 (1^+)

Supp. Table S17: **F*VQWLM$^{\$}NT^{(Me)}$**

Predicted fragment structure	Amino acid sequence	Fragment type
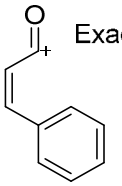 Exact Mass: 131.0491	F*	b1 - NMe_3
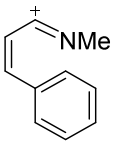 Exact Mass: 144.0808	F*	c1 - NMe_3

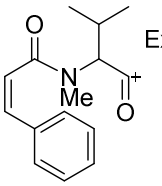 Exact Mass: 244.1332	F*V	b2 - NMe_3
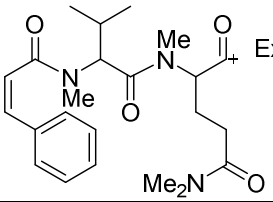 Exact Mass: 414.2387	F*VQ	b3 - NMe_3
Exact Mass: 628.3493 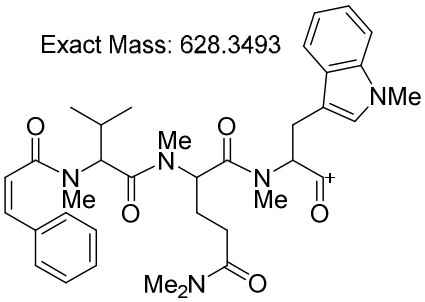	F*VQW	b4 - NMe_3
Exact Mass: 755.4491 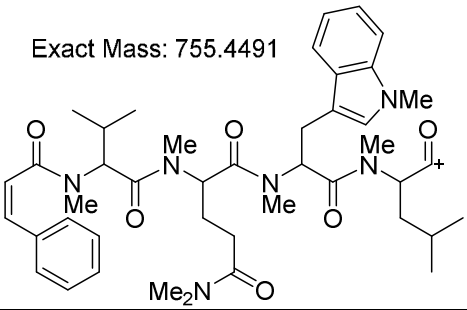	F*VQWL	b5 - NMe_3
Exact Mass: 908.5604 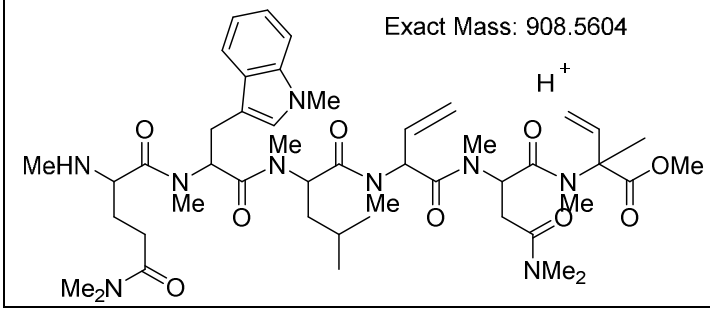	QWLM$NT	y6 - SMe - Me

	F*VQWLM$NT - Me	
	F*VQWLM$NT(Me)	
* - loss of NMe_3 $ - loss SMe		

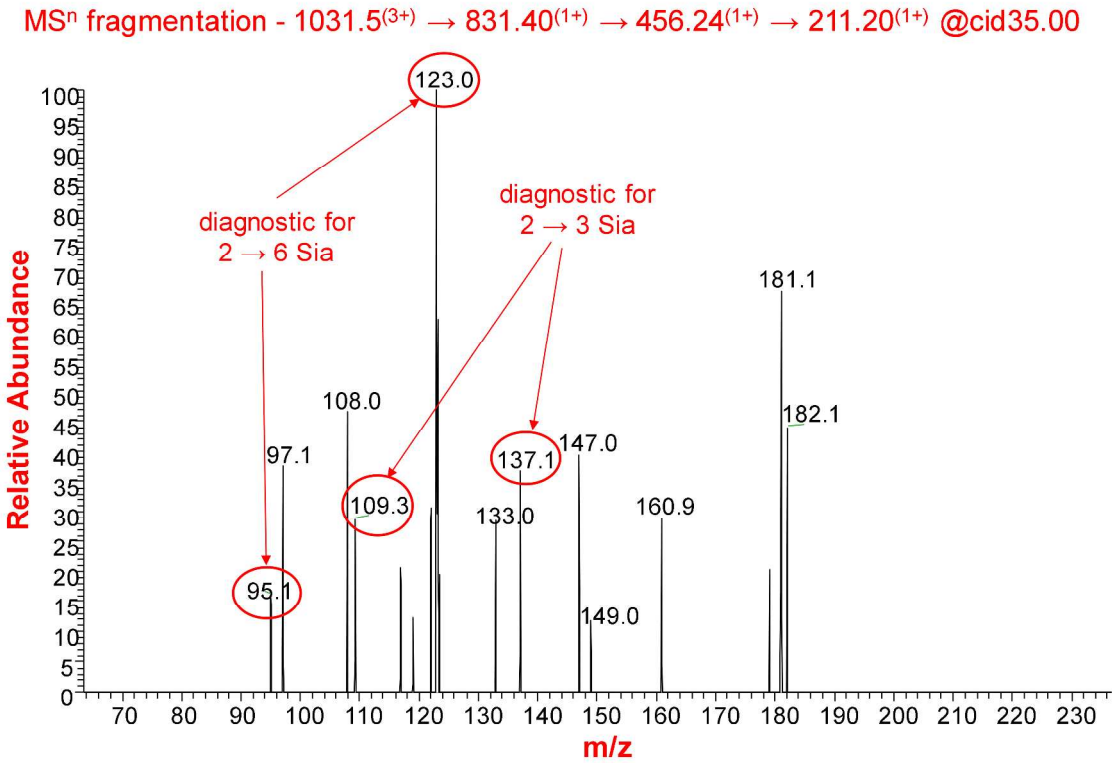

Supp. Figure S26: Identification of terminal sialic acid linkage isomers on human transferrin by MS^n analysis. CID MS^5 spectrum of permethylated di-antennary di-sialylated *N*-linked glycopeptide $N^*K^{(Me)}$ from the pronase digest of transferrin showing the presence of both α 2,3 and α 2,6 linked sialic acid (lithium adducts).